UNIVERSITY OF ALBERTA

Controls on Pore Water Arsenic in a Weathered Marine Shale under Aerobic Conditions

BY

TRACY DANIEL MULOIN

A THESIS SUBMITTED TO THE FACULTY OF GRADUATE STUDIES
AND RESEARCH IN PARTIAL FULFILLMENT OF THE REQUIREMENTS
FOR THE DEGREE OF MASTER OF SCIENCE

IN

SOIL SCIENCE

DEPARTMENT OF RENEWABLE RESOURCES

EDMONTON, ALBERTA

FALL 2002

National Library of Canada
Acquisitions and Bibliographic Services
395 Wellington Street
Ottawa ON K1A 0N4
Canada

Bibliothèque nationale du Canada
Acquisitions et services bibliographiques
395, rue Wellington
Ottawa ON K1A 0N4
Canada

Your file Votre référence

Our file Notre référence

The author has granted a non-exclusive licence allowing the National Library of Canada to reproduce, loan, distribute or sell copies of this thesis in microform, paper or electronic formats.

L'auteur a accordé une licence non exclusive permettant à la Bibliothèque nationale du Canada de reproduire, prêter, distribuer ou vendre des copies de cette thèse sous la forme de microfiche/film, de reproduction sur papier ou sur format électronique.

The author retains ownership of the copyright in this thesis. Neither the thesis nor substantial extracts from it may be printed or otherwise reproduced without the author's permission.

L'auteur conserve la propriété du droit d'auteur qui protège cette thèse. Ni la thèse ni des extraits substantiels de celle-ci ne doivent être imprimés ou autrement reproduits sans son autorisation.

0-612-81447-5

Canada

University of Alberta

Library Release Form

Name of Author: Tracy Daniel Muloin

Title of Thesis: Controls on Pore Water Arsenic in a Weathered Marine Shale under Aerobic Conditions

Degree: Master of Science

Year this Degree Granted: 2002

Permission is hereby granted to the University of Alberta Library to reproduce single copies of this thesis and to lend or sell such copies for private, scholarly or scientific research purposes only.

The author reserves all other publication and other rights in association with the copyright in the thesis, and except as herein before provided, neither the thesis not any substantial portion thereof may be printed or otherwise reproduced in any material form whatever without the author's prior written permission.

Tracy Daniel Muloin
9351-90 street
Edmonton, Alberta
Canada
T6C-3M3

Date: August/28/2002

University of Alberta

Faculty of Graduate Studies and Research

The undersigned certify that they have read, and recommend to the Faculty of Graduate Studies and Research for acceptance, a thesis entitled Controls on Pore Water Arsenic in a Weathered Marine Shale under Aerobic Conditions submitted by Tracy Daniel Muloin in partial fulfillment of the requirements for the degree of Master of Science in Soil Science.

M. J. Dudas
Marvin J. Dudas, Supervisor

Tom Chacko

Noorallah Juma

Yongsheng Feng

Date: August/27/2002

Abstract

Soils developed from marine shale often contain elevated levels of arsenic. The source of arsenic is pyrite minerals. Oxidative weathering breaks down the pyrite minerals and potentially release undesirable levels of arsenic into the surrounding pore water. Equilibration experiments on a weathered marine shale and a mixture of marine shale and glacial till were conducted under aerobic conditions to determine how much arsenic is released into pore water and the mechanism (adsorption or precipitation) responsible for limiting aqueous arsenic concentrations. Aqueous arsenic released from the shale was below 10μg/L over a 4-month equilibration. Soluble arsenic concentrations were very low considering the high total As concentrations in the shale. Over 4X as much solution arsenic was released from the higher pH shale/till system compared to the acid shale system alone. Adsorption/desorption appears to be the mechanism that limits the concentration of aqueous phase arsenic in both the shale and shale/till systems.

Acknowledgments

First and foremost I would like to thank my supervisor Dr. Marvin Dudas. Thanks for always being helpful and supportive regardless of the "caliber" of the question or problem I had. You taught me that disproving is just as important as proving, a concept that took me a while to grasp. But most of all thanks for being such a great person. The non school talks we had in the lab about golf and the cabin will be the memories I will look back on and cherish the most. I couldn't have asked for a better mentor.

I greatly appreciate the contribution made by Dr. Salim Abboud. I do not know how I could have completed my thesis without your help. Your class taught me the thermodynamic knowledge necessary to compete this thesis. I also appreciate the tequila and cigar help. Thank you to Dr. John Duke for his support and analyses during my program, but I have to say I didn't appreciate your lethal squash boast. I would also like to thank my committee members, Drs Noorallah Juma, Tom Chacko, and Yongsheng Feng. Their suggestions and the resulting changes greatly improved the quality of my thesis.

Thank you NSERC and the faculty of renewable resources and the faculty of graduate studies and research for their financial contributions.

I would like to thank my officemate Brooke Bennett. Thanks for you're help and support throughout my program. I will miss our long talks about school and everything in between. My whole masters experience was so much more enjoyable with you to share it with. Just having a second opinion and someone to exchange ideas with, as well as having someone to listen to my crazy ideas and rants was a huge help. Most of all I have gained a new friend.

I also have to thank the "group" for their support and friendship over the last couple of years and beyond. Thanks Jeff, Marshall, Rod, Glen, and Lisa. Thanks for

providing me with needed escapes whenever I needed it, and sometimes when I didn't.

And lastly I would like to thank my wonderful wife, who has stuck by me through thick and thin. I know I would have never reached this point without her help and support over the last number of years. It is nice to have someone that always believes there is nothing in life you cannot do, especially during the times you do not believe it yourself. And thank you Phoebee and Sam.

Dedicated to the loving memory of my mother and father,
and to my beautiful wife

Table of Contents

1.0 Introduction..... 1

1.1 Arsenic in the Environment..... 2
1.1.1 History..... 2
1.1.2 Arsenic Toxicity..... 3
1.1.3 Forms of Arsenic in Soil and Water..... 4

1.2 Sources of Arsenic..... 6
1.2.1 Anthropogenic..... 6
1.2.2 Natural..... 6

1.3 Background Levels of Arsenic..... 7

1.4 Marine Shale..... 7

1.5 Solubility Controls on Arsenic..... 9
1.5.1 Arsenic Minerals and Solids-Precipitation-Dissolution Chemistry..... 9
1.5.2 Adsorption-Desorption Reactions of Arsenic Species..... 15

1.6 Purpose of study..... 17

2.0 Materials and Methods..... 19

2.1 Soil Samples..... 19

2.2 Water Samples..... 19

2.3 pH..... 20

2.4 Redox-Eh..... 20

2.5 Electrical Conductivity..... 21

2.6 Bicarbonates..... 21

2.7 Solid Phase Arsenic Concentrations..... 21

2.8 Particle Size Analysis..... 22

2.9 Scanning Electron Microscope SEM..... 22

2.10 X-ray Diffraction..... 22

2.11 Anions..... 23

2.12 Cations..... 23

2.13 Equilibration Experiments..... 24

2.14 Spiking experiments..... 25
2.14.1 Spiking experiment 1-marine shale system..... 25
2.14.2 Spiking experiment 1-marine shale and till..... 26
2.14.3 Spiking experiment 2-supersaturation..... 27
2.14.4 Spiking experiment 3-partition coefficient..... 27

3.0 Results..... 29

3.1 Routine Characteristics..... 29

3.2 Pore Water Equilibration Experiments- Shale and Shale/Till Mix..... 34

3.3 Activity Ratio Diagrams..... 45
3.3.1 pH/pE diagrams..... 45
3.3.2 Conversion of equilibrium reactions used in the construction of activity ratio diagrams (ARD)..... 47
3.3.3 Activity ratio diagrams: non-equilibrium..... 47
3.3.4 Activity ratio diagrams-equilibrium..... 53

3.4 Spiking experiment 1..... 56

3.5 Spiking experiment 2..... 56

3.6 Spiking experiment 3..... 60

4.0 Discussion..... 63

4.1 Pore water equilibration: marine shale and marine shale and till..... 63

4.2 Solubility Controls on Arsenic – Adsorption or Precipitation..... 66
4.2.1 Activity Ratio Diagrams..... 66
4.2.2 Arsenic Spiking Experiment 1..... 70
4.2.3 Spiking Experiment 2- Super Saturation..... 71
4.2.4 Spiking Experiment 3 – Partition Coefficient (Kd)..... 72

5.0 Conclusion..... 75

6.0 References..... 78

List of Tables

Table 1.	Chemical and mineralogical characteristics of the marine shale and glacial till	29
Table 2.	Concentration of solution arsenic (shale samples) and percent removal after adsorption onto ferrihydrite. Arsenic spike [ ] includes the spike and any natural background arsenic	60

List of Figures

Figure 1. A pH-pE diagram for aqueous arsenic species. Source: Dove and Rimstidt (1985)..... 5

Figure 2. Activity ratio diagram outlining the possible metal-arsenate precipitates. Source: Sadiq (1997)..... 11

Figure 3. SEM micrograph of iron sulfide particle (scale at top is 10μm)..... 31

Figure 4. SEM micrograph of jarosite minerals found in the planer voids..... 32

Figure 5. A simplified view outlining the fate of arsenic after iron sulfide oxidation 33

Figure 6. Arsenic concentration (including errors) vs. reaction time in the shale and shale/till equilibration experiments 34

Figure 7. Concentration of aqueous phase arsenic (μg/L) as a function of 1/square root of equilibration time. Analyses were taken (from right to left) at 8, 16, 32, 48, 64, and 128 days respectively. Concentration of arsenic if incubation were allowed to continue to infinite time (t = 0.00) is the Y intercept of the regression formula..... 35

Figure 8. Concentration of aqueous phase arsenic (μg/L) as a function of 1/square root of equilibration time. Analyses were taken (from right to left) at 8, 16, 32, 48, 64, and 128 days. Concentration of arsenic if incubation were allowed to continue to infinite time (t =0.00) is the Y intercept of the regression formula..... 37

Figure 9. Changes in redox (Eh) and pH over the 4-month equilibration in the shale and shale/till systems..... 38

Figure 10. Mean concentrations (with errors) of major (Na, Mg, Ca, K, Fe, and SO_4) and minor (As, Mo, Ba, Al, and Mn) solution ions in the pore water samples extracted from the shale plotted against number of days since the start of equilibration..... 40

Figure 11. Mean concentrations (with errors) of major (Na, Mg, Ca, K, Fe, and SO_4) and minor (As, Mo, Ba, Al, and Mn) solution ions in the pore water samples extracted from the shale/till plotted against number of days since the start of the equilibration..... 43

Figure 12. Eh-pH Diagram for the As-S-O-H system illustrating the most likely solution species of arsenic in the shale system. The pH/pE point measured at each of the 9 equilibration times is plotted on the graph..... 46

Figure 13. Eh-pH Diagram for the As-S-O-H system illustrating the most likely solution species of arsenic in the shale/till system. The pH/pE point measured at each of the 9 equilibration times is plotted on the graph..... 46

Figure 14. Activity ratio diagram outlining possible metal-arsenate precipitates in the shale system over the 4-month equilibration assuming non-equilibrium. Actual measured arsenic concentrations (activities) for each of the 9 equilibration times are plotted on the graph..... 49

Figure 15. Activity ratio diagram outlining possible metal-arsenate precipitates in the shale/till system over the 4-month equilibration assuming non-equilibrium. The actual measured arsenic concentrations (activities) for each of the 9 equilibration times are plotted on the graph..... 50

Figure 16. Activity ratio diagram outlining the possible iron oxide precipitate formation in the shale system. Actual measured iron concentrations (activities) are plotted on the graph for each of the 9 equilibration 52

times.....

Figure 17. Activity ratio diagram for the shale system at equilibrium (infinite time). The predicted equilibrium arsenic activity is plotted on the graph..... 55

Figure 18. Activity ratio diagram for the shale/till system at equilibrium (infinite time). The predicted equilibrium arsenic activity is plotted on the graph..... 55

Figure 19. Concentration of solution arsenic in the shale system before (which includes the arsenic spike concentration and any natural background arsenic) and the concentration of solution arsenic after the spike..... 57

Figure 20. Concentration of solution arsenic in the shale/till system before (which includes the arsenic spike concentration and any natural background arsenic) and the concentration of solution arsenic after the spike..... 57

Figure 21. Activity ratio diagram for the shale system outlining the measured arsenic concentration (activity) before (which includes the arsenic spike concentration and any natural background arsenic) and arsenic activity after the spike and any possible precipitation reactions..... 58

Figure 22. Activity ratio diagram for the shale/till system outlining the measured arsenic concentration (activity) before (which includes the arsenic spike concentration and any natural background arsenic) and arsenic activity after the spike and any possible precipitation reactions..... 59

Figure 23. The amount of aqueous solution arsenic (Cw) versus the amount of arsenic adsorbed (X) onto the newly precipitated iron oxides (ferrihydrite). The slope of the line is the partition coefficient (Kd) that represents arsenic adsorption onto the freshly precipitated ferrihydrite in the shale system..... 61

1.0 Introduction

Arsenic is a naturally occurring element found in geological materials and soils. Shale of marine origin often contains elevated levels of arsenic. Arsenic in this shale is concentrated in iron sulfide minerals, mainly pyrite and arsenopyrite. During sulfide mineral formation arsenic precipitates with iron and is incorporated into the mineral structure. The average arsenic concentration in all shales is 15 mg As/kg shale (Dudas, 1987). Marine shale is found all over the world including east and west-central Alberta. Oxidative weathering breaks down the arsenic containing pyrite/arsenopyrite minerals releasing arsenic into the surrounding pore water. In Alberta, aquifers composed of weathered marine shale supply water (and potentially arsenic) for human and animal consumption to many rural residents. Previous studies by CAESA (1997), Alberta Health and Wellness (2000), and Alberta Environment (2000) measured arsenic concentrations in surface and ground water sources throughout Alberta. All of these studies observed water sources with arsenic concentrations exceeding the Interim Maximum Acceptable Concentration (IMAC) of 25μg/L (Canadian Drinking Water Quality Guideline). Waters with elevated arsenic concentrations were associated with areas underlain by geologic formations of marine shale bedrock.

There is limited information about the concentration and mechanisms (adsorption or precipitation) responsible for controlling aqueous phase arsenic under oxidizing conditions especially for the problematic areas noted in the CAESA (1997) and Alberta Health and Wellness (2000) reports. Understanding what controls pore water arsenic concentrations is essential in predicting where elevated arsenic concentrations may occur and to help reduce concentrations in problematic systems where arsenic concentrations exceed the interim maximum acceptable concentrations.

The purpose of this project was to determine how much arsenic is released into pore water and what controls or limits these concentrations in shale material with naturally elevated levels of native arsenic. This study is meant to provide insights into the relevant geochemistry that explains why some ground waters and surface waters in Alberta have naturally elevated levels of arsenic.

1.1 Arsenic in the Environment

1.1.1 History

The earliest descriptions of arsenic date back to the 4th century B.C. In Greek times both Aristotle and Discorides described arsenic, although incorrectly. In the time of Buddha arsenic was highly valued by ancient Indians. More recently Albertus Magnus, the German Dominican Scholar (1193-1280) is credited with the discovery of elemental arsenic. He mentions arsenic in its metallic form in De Rebus Metallicis. It is believed arsenic was first prepared by western alchemists in 1651 by Basil Valentine. He described arsenic as a bastard metal similar to antimony (Meyer, 1975). The first accurate experiments on the chemical nature of arsenic were carried out by Brand in 1733. He discovered that white arsenic was in fact the oxide of the element (Hunter, 1978). The deadly nature of the gas was not realized until 1815 in Munich when a German chemistry professor named Gehlen died by inhaling a small amount. In the Middle Ages arsenic was used in cosmetics (Forbes, 1964) and was a common additive used in painting and writing in imitation gold color (Thompson, 1956). Historically arsenic has also been used in the making of mirrors (Derry and Williams, 1961) and as a fluxing agent in the making of glass (Coghlan, 1975). Arsenic has also been widely used as a medication for the past five hundred years and as recently as 1940 arsenic was used in the treatment of syphilis. Other diseases that arsenic was thought to cure are rheumatism, arthritis, asthma, malaria, trypanosome infections, tuberculosis, and diabetes (Leonard, 1991). Up until the nineteenth century arsenic was the poison of choice due to its lack of smell, taste and color (Emsley, 1985). Arsenic was also added to lamps and candles and was released slowly during burning to poison its victims (Gimlette and Desmond, 1981). In the nineteenth century arsenic was widely used as a pigment in products ranging from paper products and woven fabrics to paint and rubber products. It was also combined with copper and lead as a coloring agent in paint and wallpaper. Some suggest that Napoleons death was due to green arsenic pigments in the wallpaper (Jones, 1982). Currently metallic arsenic is used mainly in the production of alloys. Arsenic is

combined with copper and more commonly lead for use in acid batteries (Carapella, 1978). Lead is also hardened with the addition of up to 3% arsenic and then used in internal combustion engines and automotive body solders. Arsenic impregnated copper is more corrosion resistant and has a higher recrystallization temperature than pure copper. High purity gallium or indium arsenide is used in the electronics industry. Gallium arsenides are used in lasers to produce coherent light directly from electricity. Other applications include light-emitting diodes (LEDs), solar cells, infrared emitters, laser windows, and experimental lasers.

1.1.2 Arsenic Toxicity

Arsenic accumulates in the body because it is readily absorbed, and slowly eliminated. Arsenic is a known carcinogen with a dose as small as 300 mg being fatal (Riewe et al., 2000). The most common pathways of human arsenic consumption are ingestion through drinking water and to a lesser extent inhalation. Chronic arsenic ingestion and toxicity causes skin diseases, such as gangrene, keratosis, and hyperpigmentation ("blackfoot disease") (Bates et al., 1992). Other health problems associated with arsenic consumption are anemia, diabetes, nerve and blood vessel damage, and digestive disorders (Riewe et al., 2000). Recent research has found evidence that suggests various cancers of the liver, bladder, and kidneys may be the result of long term exposure to inorganic arsenic (CCME, 1999). Other health symptoms expressed from low level arsenic exposure include eczema, folic acid deficiency, and brittle deformed nails (CAESA, 1997). The current Interim Maximum Acceptable Concentration (IMAC) for arsenic in drinking water is 25 μg/L stated in the Canadian Guidelines for Drinking Water Quality (Health Canada, 1996). The United States Environmental Protection Agency has recently lowered the limit on arsenic concentrations on drinking water to 10 μg/L.

1.1.3 Forms of Arsenic in Soil and Water

Arsenic occurs mainly in inorganic form in soils. Arsenic in soil is a metalloid that can exhibit both metallic and non-metallic chemical and physical properties. Inorganic arsenic most often exists in the As^{+3} valence state under reducing conditions and As^{+5} under oxidizing conditions. Most arsenic minerals and solids are As^{+5} complexes with only a few As^{+3} solids identified or reported in the literature. Reduced arsenic (As^{+3}) is more toxic, more soluble, and more mobile than the oxidized form of As^{+5} (Webb, 1966). Elemental arsenic with a valence of 0 and gaseous arsenic in the form of volatile arsenes can also exist in nature but in limited amounts. Sadiq et al. (1997) determined that only under extremely reduced and acidic conditions will arsine gas be formed.

Both pH and pE (Eh) are important in determining chemical reactions and the nature of arsenic complexing in aqueous environments. Soil pE is a parameter that indicates the redox status of a soil and is calculated by taking the directly measured Eh value (in mV) and dividing by 59.2. This pE value expresses soil redox as the negative log of electron activity making it analogous to pH with units of moles/liter. In this way electrons can be treated as other reactants and products so that both chemical and electrochemical equilibria can be expressed by a single equilibrium constant (Lindsay, 1979). The most common forms of inorganic aqueous arsenic are $H_3AsO_3^0$ (arsenite), $H_2AsO_4^-$ and $HAsO_4^{2-}$ (arsenate). The pE (Eh) and pH diagram for aqueous arsenic species is shown in Figure 1 (Dove and Rimstidt, 1985). This diagram illustrates all of the dominant arsenic species and the pH/Eh environments in which they exist.

Vink (1996) revised this diagram and included some minor differences due to increased accuracy of thermodynamic data and better understanding of various arsenic species reactions. His diagram also includes the possible polymorphs of As_2O_3, arsenolite and claudetite. In oxidized soils the dominant solution species of arsenic depends on soil pH. Below pH 2, $H_3AsO_4^0$ is the most abundant species but natural soils with pH values in this range are very rare. As soil solution pH increases into the 2 to 7 pH range $H_2AsO_4^-$ becomes the most abundant chemical form. Soil

solutions in the pH 7 to 8 range can contain both $H_2AsO_4^-$ and $HAsO_4^{2-}$ with $HAsO_4^{2-}$ becoming more prevalent as pH increases. Arsenic is common in certain minerals and is most common in sulfide minerals. The most common primary minerals that contain arsenic are pyrite (FeS_2), arsenopyrite (FeAsS), niccolite (NiAs), loellingite ($FeAs_2$), cobalite (CoAsS), realgar (AsS), and orpiment (As_2S_3). Arsenite minerals include mispikel and loellingite.

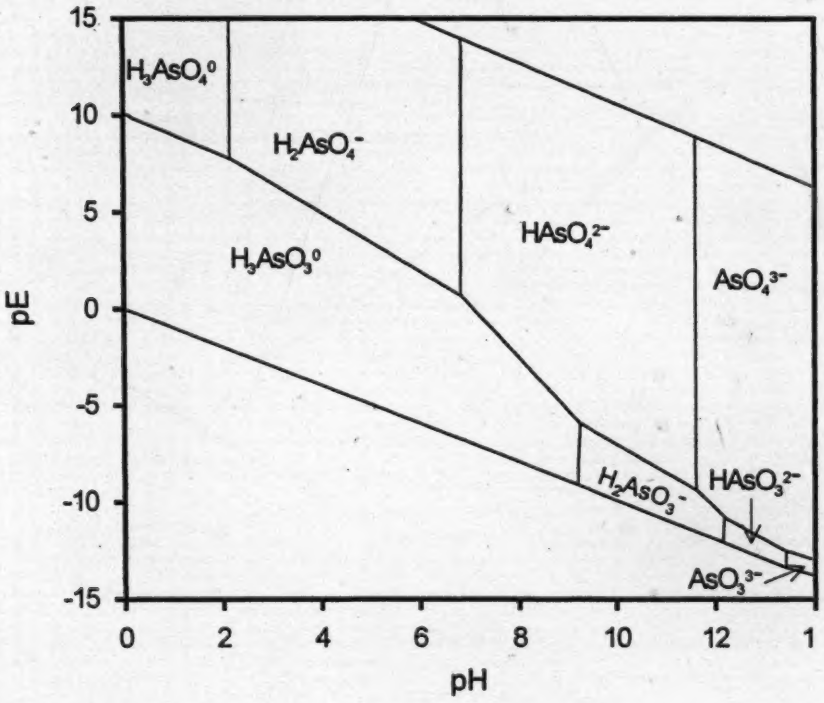

Figure 1. A pH-pE diagram for aqueous arsenic species. Source: Dove and Rimstidt (1985).

Arsenate minerals are the most common form of arsenic containing minerals found in natural systems that have been studied and reported by a number of authors including Sadiq (1997). The list of arsenate minerals is numerous. Pharmacolite ($CaHAsO_4$) and scorodite ($FeAsO_4 * 2H_2O$) are two examples. Attempts have been made to determine the most common forms of arsenic in soils. The most common arsenic forms are bound with Fe, Al, and Ca. In their study, Woolson et al. (1971) found that

Fe-As was the largest component followed by Al-As and Ca-As was the smallest component. The forms of arsenic in the soil will depend on the amounts and types of sorbing material, the pH, and the Redox status of the soil. The amount of arsenic that remains in solution is proportional to the arsenic added to a soil and inversely proportional to the iron and aluminum percentage (Woolson et al., 1973). A study by Maeda and Teshirogi (1957) found that the amount of soluble arsenic in soil increased with decreases in soil Eh and increasing pH.

1.2 Sources of Arsenic

1.2.1 Anthropogenic

Human activities have been adding arsenic to the environment for hundreds of years. These activities include the use of arsenic containing pesticides, fungicides, herbicides, insecticides, and fertilizers. The most common compounds used in these products were monosodium methylarsonate (MSMA), disodium methylarsonate (DSMA), dimethylarsinic acid (cacodylic acid), and arsenic acid. Arsenic additions have also come in the form of dust from the burning of fossil fuels and the leaching and runoff of industrial and animal wastes (Sandberg and Allen, 1975). In 1600, arsenic usage as an insecticide was mentioned in the Chinese Encyclopedia of Medicine to protect rice crops (Pascal, 1958). Until the introduction of organic pesticides in the 1940's arsenic was the dominant insecticide used by farmers and fruit growers (Nriagu and Azcue, 1990). Wood preservation salts contain arsenic and are still used today (Takahashi et al., 1983; Warner and Solomon, 1990).

1.2.2 Natural

The amount of arsenic in the various rocks depends on type, with sedimentary rocks containing the highest concentrations and igneous and metamorphic containing the least (Zou, 1986). Over 99% of all natural arsenic is found in rocks and parent material, with less than 1% in soil. It is not uncommon for sedimentary rocks to

contain up to 30 mg As/kg rock (Zou, 1986). Shale often contains elevated levels of arsenic. Shale formed in marine environments contains the highest concentrations of arsenic. Soils enriched in these minerals often contain higher than average arsenic levels. Arsenic levels in the soil will closely resemble the parent material provided there has not been appreciable redistribution from glaciation or other pedogenic processes.

1.3 Background Levels of Arsenic

It is important to know the natural background levels of arsenic to help assess environmental quality. The average amount of arsenic in the earth's crust is approximately 1.8 mg As/kg crust. The average values of arsenic in soils vary widely with levels ranging from 0.1 to 40 mg As/ kg soil with a mean of 6 mg/kg (Bowen, 1979). Backer and Chesnin (1975) also determined the mean value to be 6 mg/kg. Peterson et al. (1981) determined the average concentration of arsenic in soil to be 5 to 6 mg/kg with substantial variation between geographical regions. The average arsenic concentration in Alberta soils is 4 to 6.5 mg/kg (Dudas and Pawluk, 1980). Shale has an elevated average concentration of 14.5 mg/kg and can contain concentrations of arsenic as high as 500 mg/kg (Colbourn et al., 1975). The average concentration of arsenic in shale reported by Iimura (1981) is 13 mg/kg. A sample of five Alberta bedrock marine shale cores reported arsenic concentrations in the 10 to 20 mg/kg range (Alberta Environment, 2000).

1.4 Marine Shale

Marine shale or bedrock shale deposits are found all over the world. This material is deposited as suboxic sediments at the bottom of various water bodies such as tidal marshes, seas, and oceans. Elevated levels of arsenic are common in these sediments. The arsenic in the shale material is most often concentrated in magmatic sulfides and iron ores, the most important being pyrites, realgar, and orpiment. Pyrite minerals are formed during the diagenesis of the marine shale. During formation of

the shale arsenic is precipitated with iron where it is incorporated into the lattice sites of the mineral pyrite (FeS_2) with a Fe/As ratio of approximately 10^3 (Belzile and Lebel, 1986). When pyrite is formed arsenic often substitutes for sulfur in the mineral's structure. Arsenic held in pyrite within the marine shale is stable and unavailable to the surrounding environment provided the shale remains reduced. Oxidative weathering of marine shale results in the breakdown of the arsenic containing pyrite mineral and dissolution of arsenic. The oxidation and dissolution reaction for arsenopyrite is given by:

$$4FeAsS(s) + 13O_2 + 6H_2O \Rightarrow 4H_3AsO_4(aq) + 4Fe^{2+} + 4SO_4^{2-}$$

Upon the completion of this reaction arsenic is released into solution along with iron and sulfate. Protons (acidity) are then released as Fe^{2+} and Fe^{3+} undergo hydrolysis. Pyrite oxidation results in the release of iron, hydrogen ions, and sulfate:

$$FeS_2 + 3.5O_2 + H_2O \Rightarrow Fe^{2+} + 2SO_4^{2-} + 2H^+$$

followed by the subsequent hydrolysis of Fe and the generation of acidity (Pugh et al., 1984). The formation of various secondary minerals is another indicator of the oxidative breakdown of pyrite in shale. High quantities of gypsum, iron hydroxides, and jarosite/natrojarosite crystallize from solution in the fractures created by the H_2SO_4 dissolution of clay minerals following pyrite/arsenopyrite oxidation (Mermut et. al., 1985). An example of the reaction for iron hydroxide formation from Stahl et al. (1993):

$$Fe^{2+} + 0.25\ O_2 + 1.5\ H_2O \Rightarrow FeOOH + 2H^+$$

Lindsay (1979) gives an example of the reaction responsible for the formation of jarosite:

$$K^+ + 3Fe^{3+} + 2SO_4^{2-} + 6H_2O \Leftrightarrow KFe_3(SO_4)_2(OH)_6\ (\text{jarosite}) + 6H^+$$

Jarosite/natrojarosite is meta-stable and will gradually hydrolyze to form iron hydroxides as oxidation continues (Mermut et. al., 1985). An example of this reaction for natrojarosite:

$$2[NaFe_3(SO_4)_2(OH)_6] + 6H_2O \Leftrightarrow 6Fe(OH)_3 + 2Na^+ + 4SO_4^{2-} + 6H^+$$

The amount of jarosite and pyrite can be used to determine the amount or the stage of pyrite oxidation in shale. The co-existence of pyrite and jarosite indicates the initial stage of the oxidation process. Large amounts of jarosite and no pyrite indicates an

intermediate stage of oxidation and the breakdown and removal of the jarosite indicates the final stage of the oxidation process (Mermut et al., 1985).

In Alberta, marine shale underlies large parts of the province at varying depths. These shales were formed during the Cretaceous age in vast seas that covered large parts of what is now the province of Alberta. In Alberta this marine shale is often associated with ground water aquifers tapped with wells used for drinking water. In most cases the shale is covered by a thick mantle of glaciofluvial and glaciolacustrine deposits and is buried deep beneath the soil surface (Alberta Environment, 2000). In other areas the marine shale is near the surface in the form of large upland marine shale bedrock outcrops. An example of this is the Lower Smoky River shale of the Kaskapau formation found in the Peace River region of West-Central Alberta (Pawluk and Dudas, 1978). In areas where the shale is near the surface it is often covered by and mixed in with a thin glacial veneer forming a shale/till mixture. This is common on upland marine shale outcrops. The Josephine soil series is a natural example of one of these soil mixtures found in Alberta. The acid sulfate soils found in this area are derived from the marine shale (Dudas, 1987). A study by Alberta Health and Wellness (2000) concluded that elevated arsenic concentrations in domestic well water were associated with areas underlain with marine shale bedrock formations.

1.5 Solubility Controls on Arsenic

1.5.1 Arsenic Minerals and Solids- Precipitation-Dissolution Chemistry

Having an idea of the possible precipitation and dissolution reactions of the various arsenic minerals and solids is key in determining the environmental concentrations of arsenic. This knowledge helps in determining arsenic's speciation and possible transportation and fate in groundwater and surface water systems. Solid phase arsenic compounds formed from aqueous solutions are known as precipitation or coprecipitation reactions and are expressed as specific chemical reactions. Conversely, the breakdown of these solid phase crystalline or amorphous precipitates

into dissolved aqueous components is termed dissolution. There are many solid phase precipitate minerals of arsenic. These precipitation-dissolution reactions and the resulting solid phase compounds determines how much arsenic is in the solid phase and how much is in the dissolved phase. There are a number of factors that determine what precipitate may form and the nature of the reaction. The concentration of solution arsenic and the other metal ions that arsenic could form precipitates with is an important factor in determining the likelihood of chemical precipitation reactions. Both pH and Redox potential (Eh) are important in determining reaction rates. There is limited thermodynamic data on the equilibrium reactions of the various arsenic minerals and solids. In the past a great deal of the thermochemical data on arsenic has been unreliable. Sadiq and Lindsay (1981) reviewed the existing data and found many flaws.

Once released into solution, hydrolysis and coprecipitation can result in the formation of secondary arsenate minerals. Aqueous arsenic most often reacts with hydrous iron oxides and other metals such as cobalt, nickel, lead, and zinc.
The thermodynamic solubility of arsenic solids has been reported by a number of authors with the most recent and comprehensive list being reported by Sadiq (1997). Some of the more important equilibrium reactions and constants (log K^o) as reported by Sadiq (1997) are:

Solid species of arsenic:

$AlAsO_4(s) + H^+ \Leftrightarrow Al^{3+} + HAsO_4^{2-}$ Log $K^o = -4.70$

$Ba_3(AsO_4)_2(s) + 2H^+ \Leftrightarrow 3Ba^{2+} + 2HAsO_4^{2-}$ Log $K^o = -26.50$

$Ca_3(AsO_4)_2(s) + 2H^+ \Leftrightarrow 3Ca^{2+} + 2HAsO_4^{2-}$ Log $K^o = -1.91$

$Cd_3(AsO_4)_2(s) + 2H^+ \Leftrightarrow 3Cd^{2+} + 2HAsO_4^{2-}$ Log $K^o = -8.97$

$FeAsO_4(s) + H^+ \Leftrightarrow Fe^{3+} + HAsO_4^{2-}$ Log $K^o = -9.45$

$Mn_3(AsO_4)_2(s) + 2H^+ \Leftrightarrow 3Mn^{2+} + 2HAsO_4^{2-}$ Log $K^o = -8.51$

Solution species of arsenic:

$HAsO_4^{2-} + H^+ \Leftrightarrow H_2AsO_4^-$ Log $K^o = 6.94$

$H_2AsO_4^- + H^+ \Leftrightarrow H_3AsO_4^0$ Log $K^o = 2.24$

It is important to realize these thermodynamic values were derived at standard conditions, meaning 25°C, one atmosphere pressure, and zero ionic strength. These

conditions are almost always different than those found in soil solutions. Soils have a high degree of heterogeneity and soil solution chemical properties are highly variable. Both of these facts limit the usefulness of this data. Traditional precipitation reactions assume all solid phases formed are in their standard states. This assumption is often invalid in soil solutions. Keeping in mind the limitations mentioned above, this thermodynamic data is still useful to help predict trends, boundary conditions, and to present guidelines of chemical forms of arsenic in solution. Sadiq (1997) also determined the thermodynamic solubility isotherms using activity ratio diagrams for both arsenate and the less common arsenite solid phases. The results of the arsenate

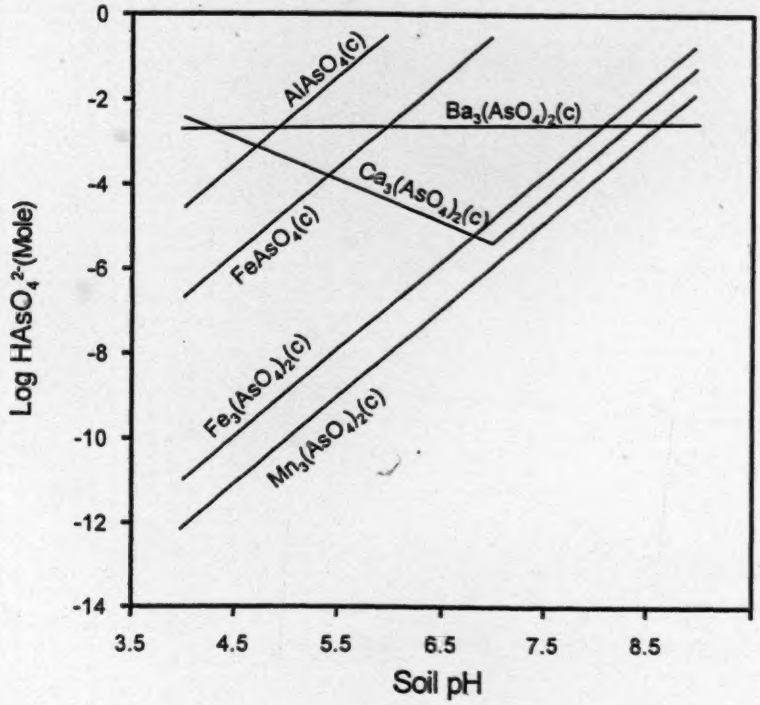

Figure 2. Activity ratio diagram outlining the possible metal-arsenate precipitates. Source: Sadiq (1997).

activity ratio diagram are shown in Figure 2. The graph represents a generalized system where the activities of the solution ions other than arsenic are in equilibrium and are controlled by various solid minerals phases. The activities of Al, Ba, Ca, Fe,

and Mn were based on the thermodynamic information from Lindsay (1979) and the equilibrium reactions in Sadiq (1997). For example Ca^{2+} activity is controlled (and is assumed to be in equilibrium with) calcite and Al^{3+} activity is controlled by gibbsite. No ion concentrations were used in the construction of this diagram. The more soluble the compound the higher the solubility line. The least soluble solid precipitate is the most likely compound to form and is represented by the lowest line provided the precipitating cation is present in the required quantity. An arsenic activity above the lowest solubility line indicates arsenic over-saturation. In this case arsenic precipitation of the metal-arsenate corresponding to the lowest precipitate line should occur. This precipitation will remove solution arsenic and drop the arsenic concentration back down to the lowest line. An arsenic concentration on or close to the lowest equilibrium line indicates a system in equilibrium. Arsenic concentrations below the line indicates under-saturation and no precipitates should form. The calculations by Sadiq show that the arsenates of Cd, Ni, Pb, Cu, and Zn were more soluble than the $Ca_3(AsO_4)_2$ solid precipitate and were not plotted on the graph. The solids of $Mn_3(AsO_4)_2$ and $Fe_3(AsO_4)_2$ will produce aqueous arsenic concentrations that are very similar to each other. These compounds have the lowest solubility in the acidic pH range and increasing solubility as the pH increases. The closeness of the Ca and Mn arsenate lines in the alkaline pH range signifies that either one could form in alkaline soils. Arsenates of Fe (Fe^{+3}) and Al are too soluble to form in any alkaline soils. In acidic soils the Ca and Mn arsenates are in equilibrium with their respective carbonates that are not stable in acidic soils and are unlikely to form. According to Sadiq, in very acidic soils, $FeAsO_4$ and $AlAsO_4$ are the most likely solid forms of arsenic to precipitate provided there is sufficient arsenic in solution. There have been a number of studies investigating the validity of the thermodynamic predictions noted above. Robins (1981) composed activity ratio diagrams for $FeAsO_4$, $Ca_3(AsO_4)_2$, and $Mg_3(AsO_4)_2$ using the most up to date free energy data available at the time. The study concluded that these three metal arsenates have much higher solubility in the area of minimum solubility than was previously thought. This study indicated that the minimum solubility for $FeAsO_4$ is just above pH 2 and the activity of arsenic in solution is about $1*10^{-3}$ molal. Any activity of arsenic below this $1*10^{-3}$ molal and

$FeAsO_4$ should not form. Any shift above or below pH 2 and the concentration of solution arsenic needed to precipitate $FeAsO_4$ increases rapidly. Robbins (1981) also found that even small concentrations of carbonates would increase the solubility of calcium and magnesium arsenates by as much as two orders of magnitude. A study by Dove and Rimstidt (1985) looked at scorodite ($FeAsO_4$) and its mode of formation and persistence in nature. This study determined that scorodite is an orthorhombic iron arsenate that is a weathering product commonly associated with arsenic-bearing ore deposits. This study suggested that the presence of scorodite controls arsenate levels in contaminated waters. Dove and Rimstidt also determined that scorodite is metastable under most conditions and tends to dissolve incongruently, forming iron hydroxides which then releases arsenate into solution. This study concluded that scorodite is stable only if the pH is less than 1.5 or if the arsenate activities are greater than 0.01 molal. In the moderately acidic pH range above pH 1.5 goethite is less soluble and is more likely to form provided the activity of arsenate is below 0.01 molal. The formation of scorodite is a multiple step process starting with the oxidation and breakdown of arsenopyrite at low pH. This breakdown produces high arsenate and iron activities leading to the next step of scorodite precipitation. A final step of scorodite breakdown was observed, but only if pH increased, resulting in iron hydroxide and aqueous arsenate. This process is shown below:

$$FeAsS(aspy) + 13Fe^{3+} + 8H_2O \Rightarrow 14Fe^{2+} + SO_4^{2-} + H_3AsO_4 + 13H^+$$

$$Fe^{3+} + H_3AsO_4 + 2H_2O \Leftrightarrow FeAsO_4{*}2H_2O(scor) + 3H^+$$

The ferric iron is produced and regenerated by Ferrooxidans bacteria.

$$Fe^{2+} + 1/4O_2 + H^+ \Rightarrow Fe^{3+} + 1/2H_2O$$

Ferrooxidans bacteria oxidize Fe^{2+} to produce Fe^{3+} that allows arsenopyrite oxidation at low pH. Past studies have shown that these bacteria live and thrive in high arsenic environments and catalyze arsenopyrite oxidation. The final step resulting in the production of iron oxides or hydroxides occurs if the pH of the reacting environment were to increase:

$$FeAsO_4{*}2H_2O(scor) \Rightarrow FeOOH + H_2AsO_4^- (aq) + H^+$$

Vink (1996) constructed a revised activity ratio diagrams for the As-Fe-O-H-S system using both Eh and pH at 25°C and 1 atmosphere of total pressure. This study indicated the range in which scorodite is stable extends throughout the acidic pH range from approximately 1 to 4.5 under moderate (200 to 800 mV) to strong (1000 to 1200 mV) oxidizing conditions. These finding are similar to Dove and Rimstidt (1985) although the stability range for scorodite was larger in the Vink (1996) study. There are a number of other iron-arsenate solids such as kaatialaite, kankite, pitticite, and angelellite according to Raade et al. (1984). There is a limited amount of knowledge and thermodynamic data on these compounds. Pitticite ($FeAsO_4$*4.5-5 H_2O) is unique because it is X-ray amorphous.

Coprecipitation is another reaction responsible for removing arsenic from solution. This is a reaction involving the simultaneous precipitation of a compound in conjunction with other compounds (Sposito, 1981). The result is a solid solution composed of more than two ions. Coprecipitation is a highly significant process affecting trace minerals in soils. This process has not been extensively studied and generally is not well understood due to the complexity of the reactions involved. One broad category of coprecipitation involves adsorption. When diffusion within the precipitate is not possible for various cations or anions, these ions can still coprecipitate by an adsorption process. This has been reported during the formation of iron and aluminum hydrous oxides. With the correct pH, various metal ions (cations, anions, and oxyanions) can adsorb onto the surface of the precipitated oxides. Because these metals can not diffuse freely into the bulk solid a true solid solution is not formed. Conditions that favor this reaction would be rapid precipitation and pronounced supersaturation (Sposito, 1981; Bohn and Bohn, 1986).

Sadiq (1997) has studied arsenic solubility in soil systems extensively and found through the use of thermodynamic calculations that in oxic, acidic, and suboxic soils iron-arsenate should control arsenic solubility. In addition, if the pH + pE of the soil is greater than 9 then the As^{+5} aqueous species (H_XAsO4^X) are most likely. Sadiq and Alam (1996) looked at dissolved arsenic in groundwater samples in Eastern Saudi Arabia and constructed thermodynamic activity ratio diagrams for the important arsenate solids. Activities of the dissolved species of arsenic were also calculated.

The observed activities were lower than the thermodynamically calculated calcium-arsenate values but the general trend observed in the measured values mirrored the theoretical values. Lack of reliable thermodynamic data for these metal arsenate's was the cause of these discrepancies and precipitation reactions that involve $Ca_3(AsO_4)_2$ were thought to control arsenic groundwater concentrations. Sadiq went on to hypothesize a three-step process that combines both solid phase formation and adsorption of As onto solid colloidal surfaces to help better represent the fate of arsenic in soil and groundwater systems. This theory is similar to the coprecipitation adsorption reaction described earlier.

1.5.2 Adsorption-Desorption Reactions of Arsenic Species

Adsorption of aqueous arsenic onto metal oxides and clay minerals is a major geochemical attenuation mechanism in pore, ground, and surface waters. Numerous studies have been conducted that describe the processes involved in arsenic adsorption onto various oxides in aerobic systems. Immobilization of arsenic in soils is due primarily to its sorption on hydrous oxides of Al, Fe, and Mn (McGeehan, 1996, McGeehan et. al., 1994, and Pierce et. al., 1982). The oxidation state and pH are important in understanding the adsorption characteristics of aqueous arsenic species. Adsorption of arsenic oxyanions occurs primarily via a specific adsorption (ligand exchange) mechanism (McGeehan et. al., 1994). Arsenate adsorption generally increases with decreasing pH, with adsorption maxima occurring near pH 4 on amorphous iron hydroxides (McGeehan, 1996).

A study by Pierce and Moore (1982) looked at isotherms for arsenic adsorption onto amorphous $Fe(OH)_3$. The study found a linear declining pattern with increasing pH at higher solution arsenic concentrations and arsenate adsorption maximum at about pH 4.

The adsorption of arsenate on ferrihydrite was studied by Raven (1998). He found that adsorption is fast at low pH and low arsenic concentrations. Adsorption occurred from pH 3.8 to 7.4, declining rapidly at higher pH. These results were similar to Pierce and Moore (1982).

Another study by Bowell (1994) experimentally developed Kd values for arsenate adsorption onto various iron oxides (goethite, hematite, and lepidocrocite). He found adsorption maxima in the pH 5 to 7 range and maximum Kd value of 10, 000 L/kg for goethite and a minimum Kd value of 35 L/kg for hematite.

Waychunas et al. (1993) looked at the surface chemistry of adsorbed and coprecipitated arsenate. They concluded the adsorbed arsenate mainly forms an inner-sphere bidentate complex and found no evidence of precipitation of any iron-arsenate compounds on the surface of the oxide.

A study by Wilkie and Hering (1996) concluded that arsenate adsorption decreased in the presence of sulfate, particularly in lower pH systems.

The pH dependent adsorption behavior of arsenic is due to the distribution of aqueous phase arsenic species determined by the Eh-pH status of the system under study and the development of pH dependent surface charge on the solids. Arsenic oxyanion adsorption is favored due to the coulombic attraction when the solid surfaces are positively charged (Xu et al., 1991).

Arsenic adsorption onto clays has been studied by Manning and Goldberg (1996). In this study the maximum arsenate adsorption occurs around pH 5 for montmorillonite and kaolinite and declines steeply at pH values greater than 6.5. The adsorption of arsenic onto clays (montmorillonite, kaolinite, and illite) is significant but the amount adsorbed is over an order of magnitude less than the adsorption onto the iron hydroxide ferrihydrite (Raven, 1998; Manning and Goldberg, 1996).

Manning and Goldberg (1997) studied arsenate adsorption in three California soils. They concluded the greatest arsenate adsorption capacity was from the soil with the highest amount of citrate-dithionite extractable iron and clay. This soil had a partition coefficient or Kd of 100 L/kg. The soil with the lowest citrate-dithionite extractable iron had a Kd of only 8 L/kg.

A study by Smith et al. (1999) found a strong link between the amount of iron and aluminum minerals and/or oxides and the amount of arsenate sorption. Smith et al. (1999) determined Kd values for the 10 soils used, with values ranging between 1.7 and 62 L/kg with larger Kd values being associated with soils with higher concentrations of iron minerals.

A report by the USEPA (1990) looked at aquifer material properties and the pH dependency of partition coefficients (Kd) with respect to arsenate. Arsenate concentrations ranged from 3 to 10 mg/L with an equilibration period of 48 hours. The highest Kd values for arsenate adsorption were in the acidic pH region with values declining as the pH became more alkaline. Actual Kd values ranged from 2 to 10000 L/kg.

1.6 Purpose of study

A great deal is known about the fate and behavior of arsenic in the environment. Adsorption and precipitation are two solubility controlling reactions that limit pore water arsenic concentrations. Almost all of the current knowledge on these reactions has been compiled using contaminated soil systems, not native natural systems.

In Alberta, there are vast areas of arsenic-rich soils. These soils are mapped as the Boundary and Josephine soil series. They contain about 10 times as much total arsenic compared to other soils in the interior plains. These soils are derived from and develop on pyrite-bearing marine shales, which have elevated levels of native arsenic. To date there have been no studies determining equilibrium pore water chemistry, including equilibrium arsenic concentrations, of these soils or the weathered marine shale. There is a distinct possibility that arsenic is elevated or concentrated in the pore water of these soils and shale. There have been no studies determining what solubility controlling reactions are responsible for removing pore water arsenic in these soils and shales that contains naturally high concentrations of arsenic. The primary objective of this study is to determine the pore water chemistry of the weathered marine shale, which is the parent material of the Boundary soil, and to determine the solubility controlling reactions responsible for limiting pore water arsenic. An equilibration experiment was conducted to accomplish this goal.

A second objective of this study is to determine the pore water chemistry of the weathered marine shale (parent material for the Boundary soil) amended with glacial till. This mixture will have a higher pH and a different chemical composition

than the native marine shale. Using this mixture provides a surrogate of other associated soil parent materials formed by the mixing of calcareous continental till from the last glaciation with the weathered marine shale that has elevated arsenic levels. The Josephine soil series is a natural example of a widespread soil developed on this kind of parent material.

The influence of the increased pH and additional attendant geochemical reactions (due to the addition of till) on the pore water chemistry of this mixture was studied with respect to the equilibrium pore water arsenic concentrations and the nature of the solubility controlling reactions. A second equilibration experiment was conducted to accomplish this goal.

A great deal of surficial material similar to this the mixture is found naturally in Alberta and northeastern British Columbia composed of glacial till and marine shale from the Kaskapau formation. Some agricultural soils are located in these deposits and are used for cultivation. These cultivated Boundary soils are often limed to raise pH resulting in a soil condition similar to the shale/till mixture of the second study. Because of these reasons it is important to understand how the arsenic pore water chemistry changes in this mixture. It is hypothesized that the increased pH will increase the pore water arsenic concentrations in this mixture. The reason for this predicted increase is due to the amphoteric nature of iron oxides and the fact more solution arsenic is needed for metal-arsenate precipitation at higher pH.

Arsenic spiking experiments were also conducted to test all theoretically predicted conclusions in the first two equilibration experiments and to determine a Kd value (partition coefficient) for arsenic adsorption onto the bulk soil and iron oxide fraction of the soil. This partition coefficient is an important component in fate transport models.

These studies will help answer practical questions like "do Boundary soils have high concentrations of water soluble arsenic", and "do these soils contribute to the release and build up of arsenic in surface and groundwater", and "does liming acid sulfate soils increase or decrease water soluble arsenic concentrations".

2.0 Materials and Methods

2.1 Soil Samples

The shale samples used in this study were collected from an outcrop of weathered pyritic marine shale belonging to the Cretaceous age Kaskapau Formation. This weathered shale is the parent geological material for the acid sulfate soils found on the upper portion of this outcrop belonging to the Boundary soil series. For the remainder of this study this material will be referred to as shale. Most accurately this material should be described as highly weathered marine shale, due to the degree of oxidation and physical weathering it has undergone. This formation is located about 60 km NW of Spirit River Alberta in Section 08-82-08 W6M. This shale is widely distributed in the area as well as the acid sulfate soils (the Boundary soil series) that have developed on it. Samples were collected on an east-facing road cut roughly 10 meters below the surface and 10 cm in from the surface of the cut. The road cut is west of the north-south running road that cuts through the middle of the outcrop. Samples were collected in late October of 2001, and were stored in large sealed plastic containers and kept in a cooler at 4°C until use. Before use the samples were air-dried and ground with a motor and pestle and sieved to less than 2mm.

The glacial till material was collected in late September of 2001. This till material was collected from the Cca horizon of a typical Orthic Black Chernozemic soil on the Cooking lake moraine north west of Tofield, Alberta. The till was collected on a south-facing hill with a moderate slope. The Cca horizon that contained about 8% calcium carbonate, was collected approximately 70 cm below the surface. All till was stored in Nalgene containers.

2.2 Water Samples

Water samples of two large surface water bodies associated with the weathered pyritic shales mentioned above were collected in late October of 2001. Sample TM-W5 was collected on the Kaskapau Formation outcrop a few hundred

meters South of the soil sampling site. Sample TM-W1 was collected 10.5 km Northwest of the outcrop. Samples were collected and stored in Nalgene plastic containers and acidified with 10 % nitric acid.

2.3 pH

The pH of the various samples was taken using a Cole-Parmer glass electrode. A Cole-Parmer digital combination pH/mV/ORP meter was used to process signals from the electrode. Electrode readings were taken in the solution phase and if the sample contained soil and solution the reading was taken at the solution-soil/shale interface. Readings were not recorded until values stabilized. Standardization was carried out using pH 4 and pH 7 buffer solutions before each sampling period. Initial pH of the acid sulfate soil was done with a 1:2 soil water solution and a 1:2 soil $CaCl_2$ solution (Carter, 1993).

2.4 Redox-Eh

The Redox potential of all samples was taken using a combination Cole-Parmer platinum electrode with a calomel reference electrode probe and a Cole-Parmer digital combination pH/mV/ORP meter. All meter Redox (Eh) numbers were recorded in mV and 245mV was added to this number to give actual redox values of the sample (Patrick et al., 1996). When taking Redox readings the probe was inserted into the solid portion of the sample and the probe was left for one hour allowing time for readings to stabilize. Standardization was conducted before the start of each sampling period using pH 4 and 7 buffer saturated with quinhydrone. Meter readings must then fall within ± 10 mV of the specified standard value (Patrick et al., 1996).

2.5 Electrical Conductivity

Electrical conductivity of the sample solutions was determined using a YSI model 31 conductivity bridge. The number (in mmhos/cm) read from the YSI bridge was converted to the sample E.C value through the formula:

$$\text{E.C of sample (mmhos/cm)} = \frac{\text{constant * reading from bridge in mmhos/cm}}{\text{KCL standard conductivity reading in mmhos/cm}}$$

The constant is 1.32 at 22°C. The KCl standard reading was taken first using a 0.01M solution. Sample values were converted to dS/m using the relationship

$$1 \text{ mmhos/cm} = 1 \text{ dS/m}$$

2.6 Bicarbonates

Bicarbonates were measured using acid titration (Bundy and Bremner, 1972). Hydrochloric acid was used at a 0.0498 M concentration. Bromocresol green was used to indicate bicarbonate, which turns yellow upon neutralization. A sample solution of 5ml was used for the titration and the concentration of bicarbonate was determined using the formula:

$$HCO_3^- = \frac{\text{(volume of acid in mL) (acid morality- moles/L) (62.0 g/mol)}}{\text{(sample volume in mL) (1L/100mL)}}$$

Routine tests for carbonates were not done due to the pH of the sample solutions. Some initial carbonate testing was done over the various sample pH ranges but no carbonate was found.

2.7 Solid Phase Arsenic Concentrations

All preliminary solid phase arsenic concentrations were determined using the SLOWPOKE (Safe Low Power Kritical Experiment) II nuclear reactor at the University of Alberta. Air-dried samples of acid sulfate soil, till, and various fractions of the weathered marine shale including iron oxide and jarosite were

analyzed in 1ml sample containers. Individual sample weights ranged from 300 to 400 mg.

2.8 Particle Size Analysis

Acid sulfate soil particle size distribution was determined using a sedimentation method. Soil was air dried and 5 g was dispersed using a Cole-Parmer ultrasonic homogenizer. Sedimentation rates were determined using Stokes Law. The clay fraction was removed following sedimentation and the remaining silt and sand fractions were separated by wet sieving. These fractions were dried and then weighed. The clay fraction was determined by taking the difference between the initial total weight and the sand plus silt fraction. Isolation of the remaining iron-sulfide minerals was also determined using sedimentation. Sedimentation rates were determined using iron-sulfide mineral density of 4.89 g/cm^3 (Deer et al., 1978) and average particle sizes estimated from similar marine shale samples found in Saskatchewan Canada (Mermut et al., 1985).

2.9 Scanning Electron Microscope SEM

Electron micrographs of the various acid sulfate fractions used for initial characterization including iron sulfides and jarosite were taken at the University of Alberta using a JEOL scanning electron microscope model JSM6301FXV. Spectral analysis of these fractions as well as any precipitates formed during spiking experiments was done using an IMIX energy dispersive X-ray detector by Princeton Gamma Tech.

2.10 X-ray Diffraction

X-ray diffraction was used to help identify precipitates and certain weathered marine shale fractions. Samples were finely ground and prepared as random power

mounts. Diffractograms were obtained using a Philips PW 1730 x-ray generator equipped with a curved crystal monochromator.

2.11 Anions

A Dionex series 4000i chromatograph was used to analyze for aqueous phase anions. This system includes a gradient pump (GPM) along with a pulsed amperometric detector (PAD). An Ionpac AS14 anion exchange column was used. This column will separate chloride, nitrate, nitrite, phosphate, sulfide, sulfite, sulfate, and thiosulfate. Samples sizes ranged from 20 to 250 mg depending on the amount of dilution required and were filtered with a 2 μm filter. All samples were run in triplicate in 5 ml sample containers. Sample checks of a pre-determined concentration were included at the start of each sampling period to determine the accuracy of the unit. If more than 10 % deviation was found from pre-determined concentration re-standardization of the unit was performed.

2.12 Cations

All aqueous phase cation concentrations were analyzed by inductively coupled plasma-mass spectrometry (ICP-MS). Analyses were conducted for Al, As, Ba, Ca, K, Fe, Mg, Mn, Mo, and Na. A Perkin-Elmer SCIEX Elan Model 5000 ICP quadrupole mass spectrometer (Thronhill, ON) was used for the analysis. All cation sample analyses were done at the Alberta Research Council, Vegreville Alberta. Submitted samples were at least 20 ml in size and were transported in 130 ml sterilized plastic containers. Samples were first filtered with a 2 μm filter and were refrigerated at 2 ^{0}C prior to transport. For a more complete explanation of the ICP-MS procedures used for analysis refer to Wu et al. (1996).

2.13 Equilibration Experiments

Two equilibration experiments were conducted using different starting materials. In the first experiment, marine shale alone was used whereas in the second experiment a mixture of marine shale and till was used in batch equilibration trials. The purpose of these experiments was to determine the equilibrium pore water chemistry in the shale and shale/till mixture and to determine the solubility controlling reaction responsible for limiting pore water arsenic. Equilibration sampling times were patterned after a study by Warren (1991).

Equilibration Experiment 1(marine shale system): Sampling times were 1, 2, 4, 8, 16, 32, 48, 64 and 128 days from the start of equilibration (samples TM-1 through TM-9). At each time, 3 samples (triplicates) were sacrificed for analysis:

9 sampling times * 3 samples sacrificed per time = 27 total samples.

Each sample consisted of 65 g of air dried and ground shale and 130 ml of distilled deionized water. All samples were equilibrated in 250 ml plastic Nalgene centrifuge bottles. All bottles were cleaned and soaked for 24 hours in a 10 % nitric acid solution prior to use. Sample bottles were partially covered with Parafilm allowing access of air and oxygen to the samples while reducing water evaporation. All samples were open systems. During the equilibrations, samples were kept in the dark. Samples were stirred daily throughout the duration of the equilibration period. Before analysis samples were stirred and centrifuged at 345 relative centrifugal forces (in g) for 20 minutes. At the end of the equilibration periods the samples were analyzed for: pH, Redox, E.C, Bicarbonates, Anions, and Cations. All procedures and methods used for the above analysis were outlined previously.

Equilibration Experiment 2(marine shale and till system): Each of the samples in equilibration experiment 2 contained 52 g of shale, 13 g of till (80% shale, 20% till) and 130 ml of distilled deionized water (samples TP-1 through TP-9). The procedures used in conducting equilibration experiment 2 were the same as the procedures used in conducted equilibration experiment 1.

2.14 Spiking experiments

A number of spiking experiments were done to test whether precipitation reactions were occurring and controlling solution arsenic concentrations in the shale and shale/till systems. Arsenic spiking was done using sodium hydrogenarsenate heptahydrate ($Na_2HAsO_4 * 7H_2O$). All samples were equilibrated in partially covered 250 ml nalgene plastic centrifuge containers. These containers were sterilized using 10% nitric acid prior to use. Initially samples contained either:

a) 65 g of shale and 130 ml of distilled deionized water

b) 52 g of shale, 13 g of till (Cca), and 130 ml of distilled deionized water.

These mixtures were incubated for a fixed amount of time based on results of the first equilibration experiments and then centrifuged at 345 relative centrifugal forces (in g) for 20 minutes. Redox, pH, bicarbonates, and E.C. readings were taken and a set volume of the solution portion of the samples was removed and filtered (2 μm) and transferred to another 250 ml plastic centrifuge container. The arsenic spike was added to this solution, in either solid or liquid form depending on the concentration of arsenic that was needed. Using solid arsenic for spiking made it easier to administer large spike concentrations. Spiking was done on the solution phase only to eliminate any adsorption reactions on any of the solid phase components of the shale or till. These solutions were partially covered and allowed to react. Before a portion of the solutions was removed for anion and cation analysis the samples were transferred to 50ml plastic nalgene centrifuge tubes and spun at 26900 RCF for 20 minutes. Finally any solution removed for anion and cation analysis was taken from the top half of the tubes and filtered with a 2 μm filter. This was done to ensure that any precipitates formed would not be included in the solutions used for anion and cation analysis.

2.14.1 Spiking experiment 1-marine shale system

In this spiking experiment, 9 samples were initially used which contained shale and water. These samples were allowed to react for 7-days in 250 ml plastic centrifuge containers. A reaction time of approximately 16 days or greater would

have been more ideal, allowing solution ions more time to stabilize (based on initial equilibration experiments). However preliminary experiments indicated an equilibration of 7 days minimizes solution Fe concentrations (solution Fe concentration reaches a maximum or spikes around 16 days), eliminating amorphous iron-oxide formation from solution, which would interfere with any possible arsenic precipitation. After the initial equilibration the pH, Redox, bicarbonates, and E.C. were determined and 90 ml of solution was filtered (2 μm), removed and transferred to another 250 ml plastic centrifuge container. These 9 solution samples were divided into 3 groups of 3 and were spiked with 4 μg/L, 25 μg/L, or 100 μg/L of arsenic. The arsenic was added as a 1ml increment in liquid form. These solutions were reacted for 8 days, transferred to 50 ml plastic centrifuge tubes and centrifuged at high speed before analysis for cation and anion concentrations. These tests were done to determine if the precipitation of a metal-arsenate was controlling solution arsenic concentrations in the aqueous phases equilibrated with the shale samples.

2.14.2 Spiking experiment 1-marine shale and till

In this spiking experiment, 9 samples were initially used containing the shale/till mixture and water. These samples were reacted for 16 days (no sharp increase or spike in Fe concentration was observed in the shale/till mixture around the 16 day equilibration time). After incubation the pH, Redox, bicarbonates, and E.C. were determined and 90 ml of solution was filtered, removed and transferred to another 250 ml plastic centrifuge container. These samples were divided into 3 groups of 3 and spiked with 4 μg/L, 25 μg/L, or 100 μg/L of arsenic. The arsenic was added as a 1ml increment in liquid form. These solutions were reacted for 8 days, transferred to 50 ml plastic centrifuge tubes and centrifuged at high speed before analysis for cations and anions. These tests were done to determine if the precipitation of a metal-arsenate was controlling solution arsenic concentrations in the aqueous phases equilibrated with the shale/till samples.

2.14.3 Spiking experiment 2-supersaturation

The initial starting samples in this spiking experiment contained either shale or the shale/till mixture and water. Theory predicts that if the concentration of solution arsenic is high enough various metal-arsenate precipitates will form. This experiment adds a large concentration of arsenic or spike to the removed solution portion of the samples to determine if these theoretically predicted precipitates form. Initially 3 shale samples were allowed to react for 4 days and 3 shale/till samples were reacted for 18 days (the reduced 4 day initial reaction time of the shale samples was due to the large increase or spike in solution Fe mentioned in section 2.14.1). After the initial reaction periods the pH, Redox, bicarbonates, E.C., anions, and cations were determined for the 6 samples. Then 60 ml of solution was filtered (2μm) and removed from each sample and transferred to another 250 ml plastic centrifuge container. These solutions were spiked with 0.1 mol/L of arsenic, added as solid sodium hydrogenarsenate heptahydrate (1.872g into each container). These samples were reacted for 8 days, transferred to 50 ml plastic centrifuge tubes and centrifuged at high speed before analysis for anions and cations. Any visible precipitates that formed were separated, dried and kept for XRD analysis and SEM analysis.

2.14.4 Spiking experiment 3-partition coefficient

The purpose of this spiking experiment was to determine how much arsenic would be adsorbed onto the newly formed iron oxide fraction of the shale. In this spiking experiment, 9 shale samples were used and initially reacted for 16 days. The samples were analyzed for pH, Redox, E.C., bicarbonates, and aqueous arsenic concentrations. The next step was to filter, remove, and transfer 90 ml of solution to another 250 ml plastic centrifuge container. This length of incubation time maximizes solution Fe concentrations and results in the formation of amorphous iron oxides on the sides of the 250 ml plastic centrifuge containers holding the transferred solution portion of the samples. Three of the samples were spiked with 26.41 μg/L of arsenic, three were spiked with 100 μg/L and the last three were spiked with 3.38

mg/L of arsenic. After spiking the samples were reacted for 16 days, transferred to 50 ml plastic centrifuge tubes and centrifuged at high speed. Solution samples were taken from the top half of the centrifuge tubes only. These samples were analyzed for anions and cations.

3.0 Results

3.1 Routine Characteristics

Routine chemical and mineral characteristics of the weathered marine shale and the glacial till are summarized in Table 1.

Table 1. Chemical and mineralogical characteristics of the marine shale and glacial till.

Characteristic		*Marine Shale*	Till(Cca)
pH ($CaCl_2$)		2.63	7.56
pH (H_2O)		2.75	7.07
Redox		600mV	483mV
E.C		2.09 dS/m	0.50 dS/m
TDS (total dissolved solids)		2320 mg/L	320**
Carbonates-$CaCO_3$ equivalent		0	8.6%****
Texture	Sand	0.33%	28%***
	Silt	39.20%	45%***
	Clay	60.10%	27%***
Clays Mineralogy		mica, hydrous mica kaolinite*	montmorillonite,kaolinite mica, chlorite****
Bulk Density		1.15-1.41 Mg/m^3*	-
CEC		16.7-23.5 cmol/kg*	13.30 cmol/kg****
Color	Bulk Soil	10YR 8/1 dry	10YR 6/6 dry
	iron oxides	2.5YR 3/6 dry	-
	jarosite	2.5Y 8/8 dry	-
Initial Solid Phase Arsenic	iron oxides	305 ug/g soil	-
	jarosite	59.4 ug/g soil	-
	sand fraction	382 ug/g soil	-
	silt fraction	21.8 ug/g soil	-
	clay fraction	34.4 ug/g soil	-
	bulk sample 1	34.8 ug/g soil	10.5 ug/g soil
	bulk sample 2	31.9 ug/g soil	-

* from Bulmer, 1987
** estimated from E.C.
*** based on manual texture
**** from Ruhman, 1979

There have been numerous past studies investigating acid sulfate soils derived from the same or similar Cretaceous marine shale used in this study (Pawluk and Dudas, 1978; Ross and Ivarson, 1981; Mermut et al., 1985; Dudas et al., 1988). This shale contains large amounts of clay, usually dark gray in color. The amount of clay (Table 1) closely matches amounts found in past marine shale studies, like the 57% found by Pawluk and Dudas (1978) and the 54-60% found by Bulmer (1987). Both of these past studies used soil from the same outcrop used in this study. The most identifiable feature of the marine shale is the low pH (2.75). Oxidation of iron sulfide minerals, specifically pyrite and arsenopyrite, release ferric hydroxides and sulfuric acid. Vegetation associated with the acid sulfate soils derived from this marine shale is often stunted or absent due to this extremely low pH. This has been observed in Saskatchewan (Mermut et al., 1985) and in Alberta (Bulmer, 1987). Due to the relationship between pH and Eh described by Lindsay (1979) and the low pH of the shale, the Eh (redox status) of the shale is extremely high.

The amount of arsenic associated with the individual particle size and mineral fractions is shown in Table 1. The amount of arsenic in the bulk sample was approximately 35 μg As/g soil. This amount falls within the range (5 to 45 μg As/kg soil) found by Dudas et al. (1988). There are large amounts of arsenic associated with the sand and the iron oxide fractions. The only remaining iron-sulfide minerals (pyrite or arsenopyrite) that have not undergone complete oxidation are contained in the sand fraction due to the high density of these minerals. These minerals are the original carriers of arsenic in the shale. These iron sulfides contain large amounts of arsenic that was captured and held in the lattice structure during its formation (Belzile and Lebel, 1986). The amount of total arsenic in the sand fraction is 382 μg As/g sand. Very little of the total iron sulfide minerals remain, due to the breakdown by oxidative weathering. The sand fraction makes up only 0.33% of the total mass, and only a small portion of this fraction still contains any iron sulfide minerals. Some of the remaining iron sulfide minerals were isolated and analyzed using the SEM. A micrograph of one of these mineral particles is shown in Figure 3. The shape of pyrite and arsenopyrite before oxidative weathering is pyramidal with smooth sides,

5-30 μm in size (Mermut et al., 1985). The mineral in Figure 3 has lost any pyramidal shape and smoothness indicating advanced oxidation.

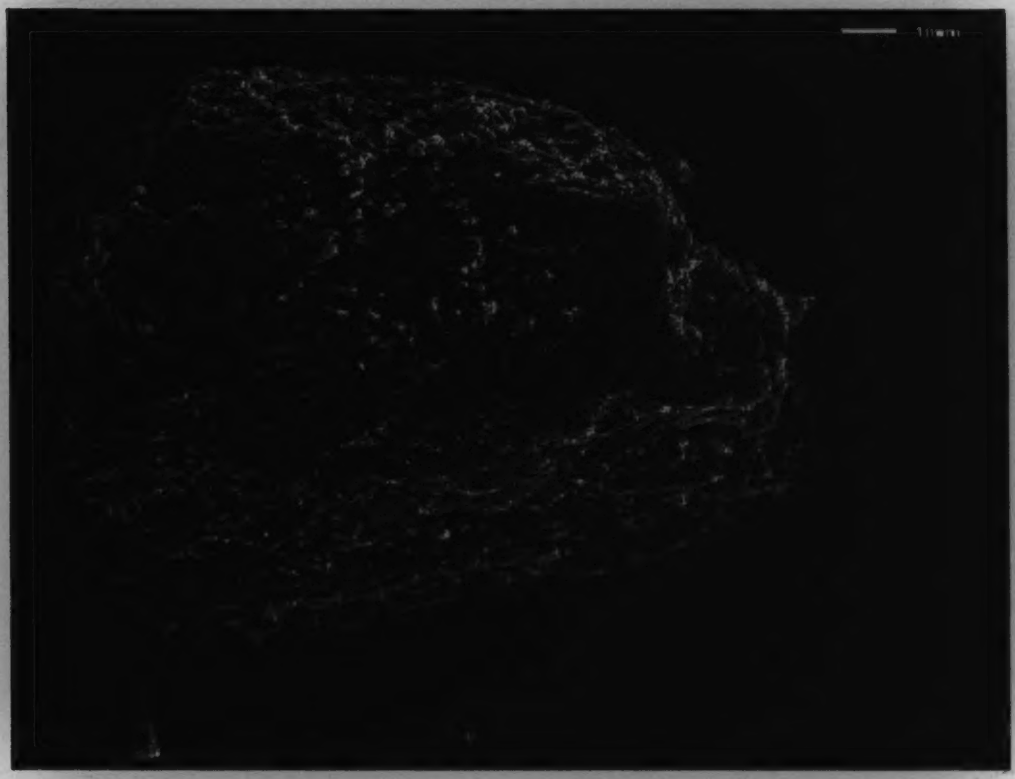

Figure 3. SEM micrograph of iron sulfide particle (scale at top is 10 μm).

The iron oxide fraction also contains elevated arsenic concentrations and is further evidence that the shale has undergone advanced oxidation. These oxides were analyzed by XRD and are amorphous in nature. Ferric hydroxide glaebules as large as pyrite crystals were common in similar shale found in Saskatchewan (Mermut et al., 1985) and could be the form of iron oxide observed here. These oxides are concentrated in planer voids created by the H_2SO_4 dissolution of clay minerals following pyrite/arsenopyrite oxidation (Mermut et. al., 1985) and are olive brown to dark reddish brown in color. These cracks allow oxygen and oxygenated water to

penetrate into the shale accelerating the oxidation process. Needle shaped gypsum crystals were also present in the voids. Gypsum is another by-product of iron sulfide oxidation. Jarosite ($KFe_3(OH)_6(SO_4)_2$) and natrojarosite ($NaFe_3(OH)_6(SO_4)_2$) were also found in the voids. These minerals form in solution from the products produced after iron sulfide oxidation. The co-existence of both iron sulfide and jarosite indicates an intermediate stage of oxidation (Mermut et al., 1985). A SEM micrograph of this mineral is given in Figure 4.

Figure 4. SEM micrograph of jarosite minerals found in the planer voids.

The jarosite is 0.1 to 1.0 μm in size and has a distinct cubic morphology. Spectral analysis conducted during the SEM session indicated jarosite whereas XRD analysis indicated natrojarosite. It appears that this material is made up of a combination of these minerals.

The possible redistribution of As after oxidative weathering of the pyritic shale (in a simplified representation) using the solid phase arsenic concentration numbers is outlined in Figure 5. Figure 5 illustrates that once arsenic is released from the iron sulfide minerals, approximately 80% of the arsenic is removed from solution by the iron oxides, 15% is removed from solution by jarosite and natrojarosite, and 5% is removed by the silt fraction. There are other fractions that will remove arsenic in this system that are not included.

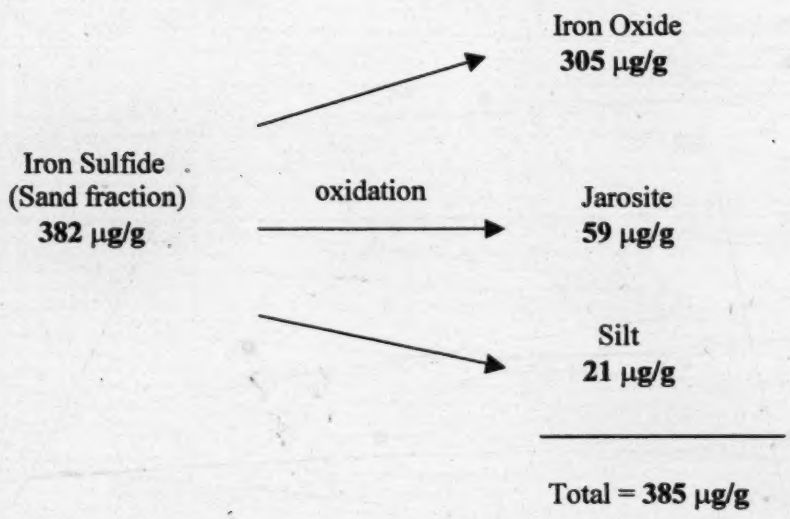

Figure 5. A simplified view outlining the fate of arsenic after iron sulfide oxidation.
* Note the clay fraction was not included due to the fact the iron oxide and jarosite minerals are the main components of this fraction that contain arsenic.

A 10-day equilibration of the glacial till was conducted to determine how much arsenic is released into solution from this material. After the 10 days only 0.7 µg/L of arsenic was released into solution. This indicates that the addition of till did not add significant amounts of aqueous phase arsenic.

3.2 Pore Water Equilibration Experiments- Shale and Shale/Till Mix.

The change over time of the mean pore water ion concentrations and other chemical parameters in both equilibration experiments (shale and the shale/till mixture) are displayed in Appendix 1. The change in arsenic concentrations over the equilibration period in the shale and shale/till systems are displayed in Figure 6.

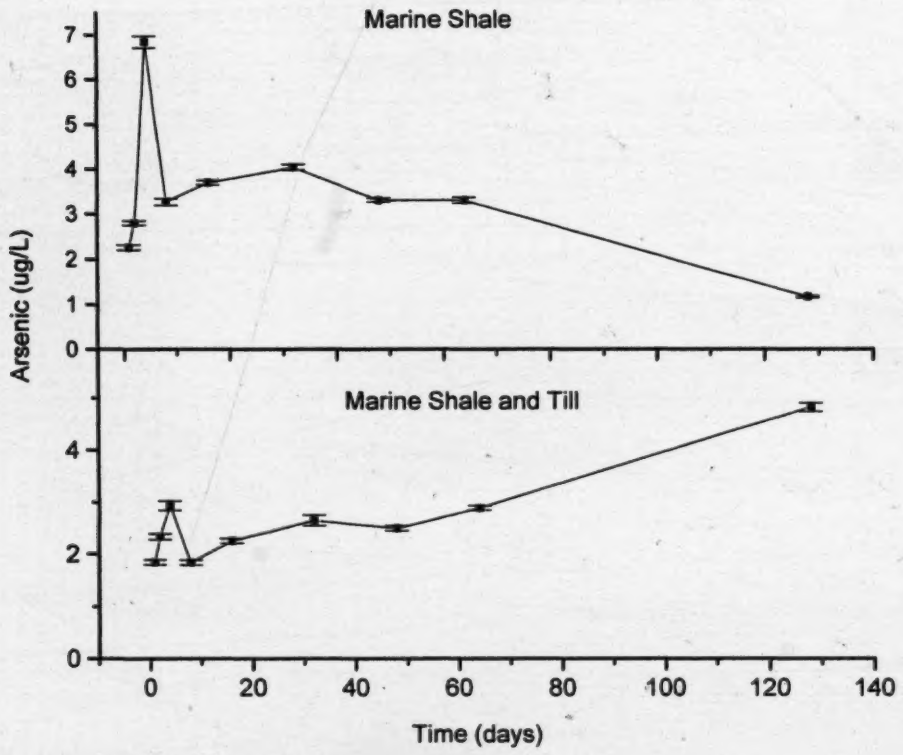

Figure 6. Arsenic concentration in pore water (including errors) vs. reaction time in the shale and shale/till equilibration experiments.

In the shale equilibration experiment, arsenic concentrations initially increase up until day 4 (reaching a maximum of 6.84 μg/L) followed by a decrease in

concentration until the end of the 4-month equilibration. At the end of the 4 months, the concentration of arsenic dropped down to 1.17 µg/L. There is an overall decreasing trend in the aqueous phase arsenic concentrations in the shale experiment. As equilibration times increase the downward trend in arsenic concentration seen in Figure 6 indicates that the concentration of arsenic should remain in the low µg/L range over longer time periods. Estimates of the aqueous phase arsenic concentration in the shale system as time approaches infinity is displayed in Figure 7 (Kittrick, 1966). This method of graphing the arsenic concentration vs. inverse square root of time provides an estimate of the equilibrium solution arsenic concentration.

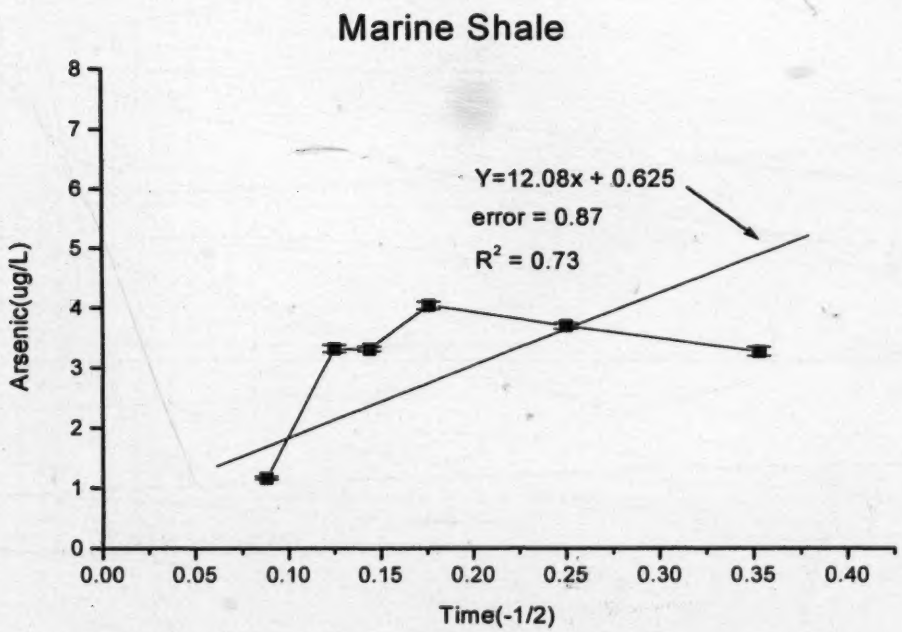

Figure 7. Concentration of aqueous phase arsenic (µg/L) as a function of 1/square root of equilibration time. Analyses were taken (from right to left) at 8, 16, 32, 48, 64, and 128 days respectively. Concentration of arsenic if incubation were allowed to continue to infinite time (t = 0.00) is the Y intercept of the regression formula.

This equilibration study looked at arsenic concentrations over a 4-month period. The kinetics of soil solutions is often slow due to the high degree of complexity and heterogeneity in these solutions. Reaching equilibrium in these solutions is often slow and it is likely that the shale and shale/till solutions have not reached equilibrium at the end of the 4-month equilibration. This approach allows predictions to be made about what the concentration of arsenic is at infinite time or when the system has reached equilibrium. Kittrick (1966) used this method to predict equilibrium ion concentrations for solutions containing only 2 ions, unlike the complex soil solutions containing multiple ions of this study. Therefore, it is important to note that any predictions of arsenic concentrations assumed to be in equilibrium are only predictions. The predicted concentration of arsenic after equilibrium has been achieved (or infinite time) in the shale system is 0.625 μg/L based on the data shown in Figure 7. Only the last 6 equilibration times were used in constructing Figure 7. The first 4 time periods (day 1, 2, 4, and 8) were excluded due to the erratic changes in arsenic concentrations over this time. The equilibrium arsenic concentration predicted from Figure 7 will change depending on how many points (corresponding to equilibration times starting from the end of the equilibration) are used in the projection to infinite time. If only the last 4 equilibration times were used (day 128, 64, 48, and 32), a more linear relationship is the result, as well as a better regression fit. The reason for this better fit is due to the similar trend in arsenic concentration changes over the last portion of the equilibration compared to the first part of the equilibration (Figure 6). The predicted arsenic concentration at equilibrium using the last 4 equilibration times is −1.24 μg/L. A negative concentration is obviously impossible. The reason this number is so low is due to the pronounced downward trend in arsenic concentration over the last 4 equilibration time periods (day 32, 48, 64, and 128) as seen in Figure 6. The result is a steep (positively) sloping regression line that crosses the y-axis below zero resulting in the negative concentration. Taking both of these values into account it appears that the predicted equilibrium solution arsenic concentration is between 0.0 μg/L and 0.6 μg/L. The concentration of aqueous phase arsenic in the shale/till experiment initially rises up until day 4 (a rise of only 1 μg/L), drops, and then steadily increases

until the end of the 4 month equilibration period (Figure 6). Arsenic concentrations increase from 1.85 μg/L (day 1) to 4.82 μg/L (day 128). The trend in arsenic concentration change in the 2 equilibration experiments (shale and shale/till mix) is nearly identical for the first 7 equilibration times (day 1, 2, 4, 8, 16, 32, and 48) (Figure 6) and is opposite over the last 2 months of the equilibration. In the shale/till equilibration, arsenic concentrations continue to increase until the end of the equilibration period. The predicted equilibrium arsenic concentration (arsenic concentration at infinite time) is displayed in Figure 8.

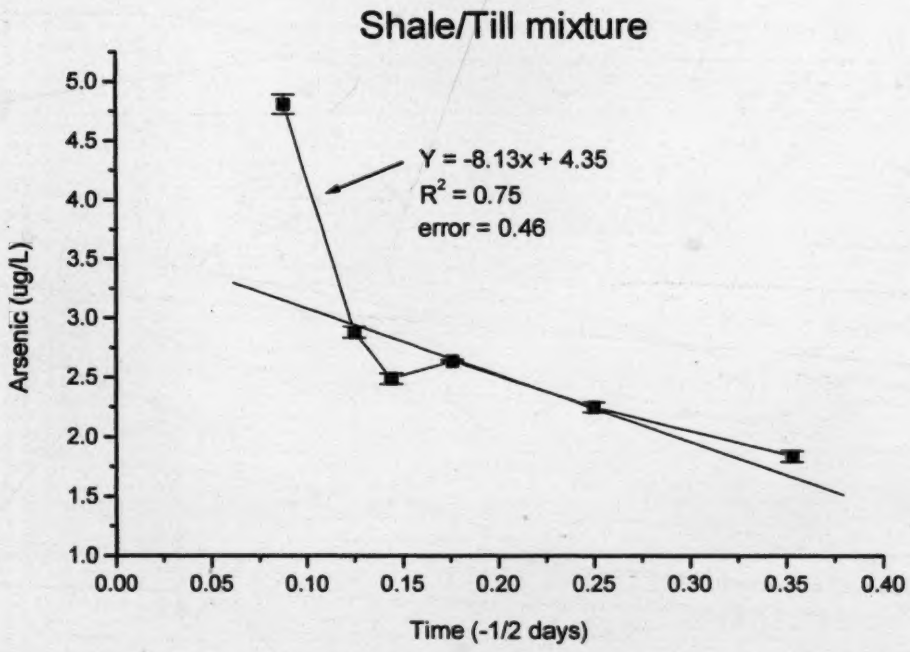

Figure 8. Concentration of aqueous phase arsenic (μg/L) as a function of 1/square root of equilibration time. Analyses were taken (from right to left) at 8, 16, 32, 48, 64, and 128 days. Concentration of arsenic if incubation were allowed to continue to infinite time (t =0.00) is the Y intercept of the regression formula.

The last 6 equilibration times were used in the construction of Figure 8. These times were used because the trend or change in arsenic concentration over the last 6 time periods is similar (increasing) which results in a reasonable linear relationship. The

concentration of equilibrium arsenic (infinite time) is 4.35 μg/L. As mentioned previously, the concentration of arsenic at equilibrium will change depending on how many points (equilibration time periods) are used. The graph could have also been constructed using the last 2, 3, or 4 time period data points, which would result in a larger predicted equilibrium arsenic concentration value. The larger predicted equilibrium arsenic concentration value is due to the steeper increase in solution arsenic concentration towards the end of the 4-month equilibration. Concentrations

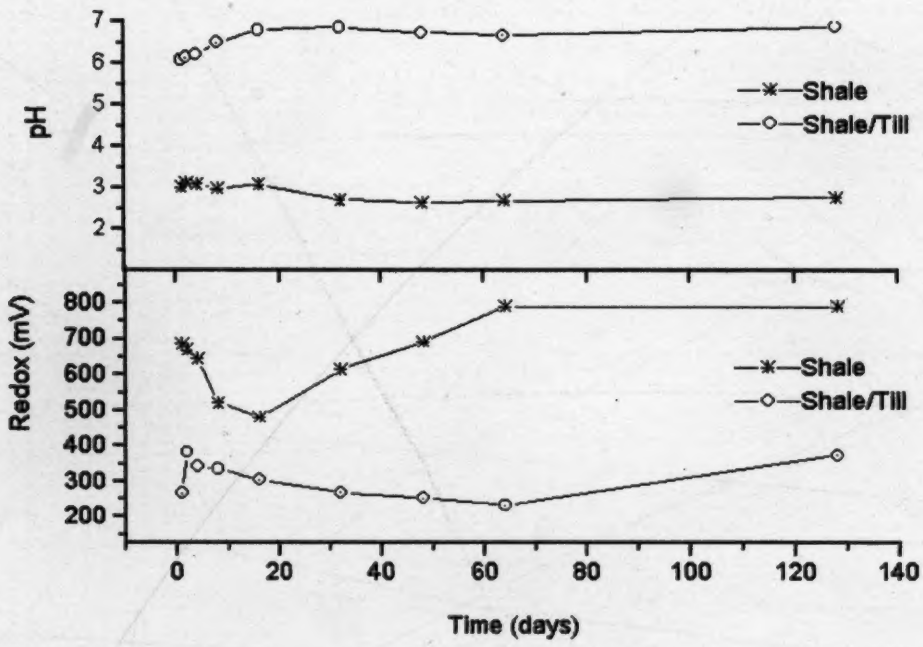

Figure 9. Changes in redox (Eh) and pH over the 4-month equilibration in the shale and shale/till systems.

of arsenic rose sharply over the last 2 months (days 64 and 128) in the shale/till systems (Figure 6). The resulting equilibrium concentration of arsenic (at infinite time) if only the last 2 points (day 64 and 128) were plotted is 9.4 μg/L. This number represents the largest predicted equilibrium arsenic concentration because it is based

on the time period with the steepest increase in arsenic concentration over the 4-month equilibration. The predicted equilibrium solution arsenic concentration in the shale/till systems is between 4.3 and 9.4 μg/L.

Changes in pH and redox (Eh) over the equilibration period are displayed in Figure 9. There is very little change in pH in both experiments, with a maximum change (increase) of 0.8 pH units (from pH 6.1 to 6.9) observed in the shale/till system over the entire 4-month equilibration period. This increase in pH with time indicates the consumption of acid. A drop in pH was observed in the first equilibration experiment (shale only) from 3.01 to 2.77 (0.24 pH units total). This drop in pH in experiment 1 is likely due to the breakdown of any remaining iron sulfide mineral material, accelerated by the addition of water, resulting in the production of sulfuric acid expressed in the equation (Pugh et al., 1981):

$$FeS_2 + 15/4O_2 + 7/2H_2O \Leftrightarrow Fe(OH)_3 + 2H_2SO_4$$

The redox (Eh) in the first equilibration (shale only) starts off approximately 420 mV lower than the second equilibration (shale/till). This difference in redox is likely due to the large initial difference in pH and the strong relationship between pH and redox. Both pH and redox (Eh) are necessary to specify the redox status of aqueous environments (Lindsay, 1979). Redox values fluctuate in both experiments over the majority of the equilibration period. At the end of the 4-month incubation, the difference in redox values between the 2 experiments was again approximately 420 mV (Figure 9).

The concentration of the major ions (Na, Mg, Ca, K, Fe, and SO_4) and minor ions (As, Mo, Ba, Al, and Mn) in the solution phase plotted against equilibration time in the shale equilibration is presented in Figure 10. The plot of arsenic concentrations over the 4-month equilibration indicates equilibrium conditions are not established in the experiments of this study. The concentration of arsenic over the last 2 months of the equilibration continues to change (decrease). The change in concentrations of the other minor and major ions in solution indicates a system that is in equilibrium or very close to it. The concentrations of Al, Ba, Fe, K, Mg, and SO_4 all remain relatively constant over the latter part of the equilibration. Only the concentration of

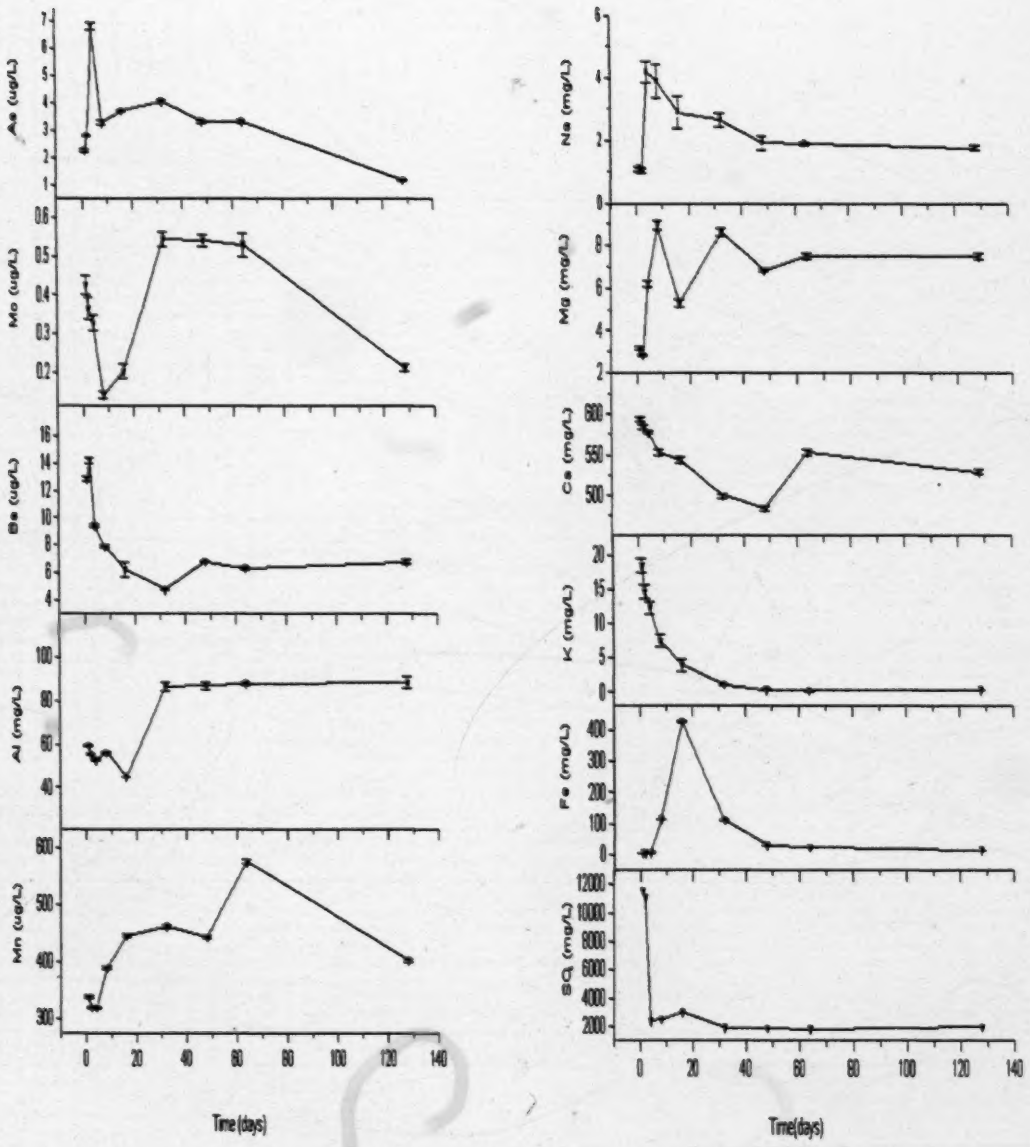

Figure 10. Mean concentrations (with errors) of major (Na, Mg, Ca, K, Fe, and SO_4) and minor (As, Mo, Ba, Al, and Mn) solution ions in the pore water samples extracted from the shale plotted against number of days since the start of equilibration.

Mn is still substantially changing (and Ca to a much lesser degree) at the end of the equilibration, indicating this ion has not reached a state of equilibrium. The only ion that mimics the change in arsenic concentrations over the last part of equilibration is Mo. The common form of molybdenum (in the pH and Eh range of this study) in solution is the oxyanion molybdate (MoO_4^{2-}). This ion has a net negative charge and should act in a similar way to aqueous arsenic that also has an oxyanion form in solution ($H_2AsO_4^-$). A recent study by Alberta Health and Wellness (2000) reported a strong relationship in the adsorption and desorption behavior between aqueous arsenic and molybdenum onto the positively charged surfaces of Fe oxides. This observed relationship between As and Mo in solution may indicate that adsorption/desorption reactions are controlling As and Mo solution concentrations and not precipitation. If precipitation reactions were controlling or limiting solution arsenic, then the solution cation that arsenic precipitates with should mirror any arsenic concentration changes. This was not observed as the concentration of most solution ions were stable (in equilibrium) at the end of the equilibration and not decreasing like solution arsenic concentrations. The sharp increase in arsenic concentration on the 4th day is likely due to competitive desorption from the large amounts of sulfate ions present (sulfate concentrations are over 100,000X higher than arsenic) at the start of the equilibration. Sulfate like arsenic has a net negative charge and will compete with arsenic for any positively charged adsorption sites. These initially high concentrations of SO_4 (11556 mg/L), and to a lesser extent K and Ca, are likely due to increased mineral dissolution during the air-drying process. Sulfuric acid produced during oxidation is concentrated in the pore water facilitated by evaporation of water during the drying process. This increased acidity dissolves minerals in the samples forming efflorescent salts that rapidly re-dissolve during re-wetting (Warren, 1991). These are likely sulfate salts of the major ions precipitated during drying. A large amount of jarosite (and natrojarosite) was initially found in the marine shale. The jarosite occurred in its characteristic yellow efflorescence on structural faces and in cracks and pore spaces. Jarosite (and natrojarosite) is meta-

stable in the pH range of the shale equilibration. It will hydrolyze, resulting in the formation of ferric hydroxides (Mermut et al., 1985) represented by the reaction:

$$2[NaFe_3(SO_4)_2(OH)_6] + 6H_2O \Leftrightarrow 6Fe(OH)_3 + 2Na^+ + 4SO_4^{-2} + 6H^+$$

This breakdown was observed in the changes of solution ion concentrations in the shale experiment. There was a large increase in solution iron at the 16-day mark (a 420 mg/L increase from the start of the incubation), along with an increase in the sulfate concentration at the same time (652 mg/L increase). Jarosite commonly contains arsenic, and a small increase in arsenic concentration was also observed around the same time. Solution iron concentrations dropped off after the jarosite breakdown, forming the iron hydroxide ferrihydrite. This was observed over the course of the experiment, as an orange/red precipitate formed on the sides of the sample containers after the 16-day mark. This material was harvested after the samples were sacrificed and the precipitate was analyzed using XRD. The results indicated an amorphous compound, consistent with a ferrihydrite iron oxide. Ferrihydrite has been shown to form in systems that undergo rapid or extreme oxidation (Schwertmann et al., 1989) similar to conditions found in the shale experiment. An activity ratio diagram was constructed to illustrate the ferrihydrite formation and will be presented in the next section. The concentration of arsenic steadily decreases after the ferrihydrite formation which further indicates that adsorption is the main reaction controlling solution arsenic concentrations.

The concentration of the major ions (Na, Mg, Ca, K, Fe, and SO_4) and minor ions (As, Mo, Ba, Al, and Mn) in the solution phase plotted against reaction time in the shale/till equilibration is presented in Figure 11. It appears that arsenic has not reached a state of equilibrium at the end of the 4-month equilibration as indicated by the trend in arsenic concentration over time. The overall system equilibrium can be inferred from the changes near the end of the equilibration in the other solution ions. There is no clear trend in the concentration changes of the other solution ions. The Ba, Mn, Mg, and Ca ions are relatively stable at the end of the equilibration indicating equilibrium for these ions and their solid phases. However, the concentrations of Al,

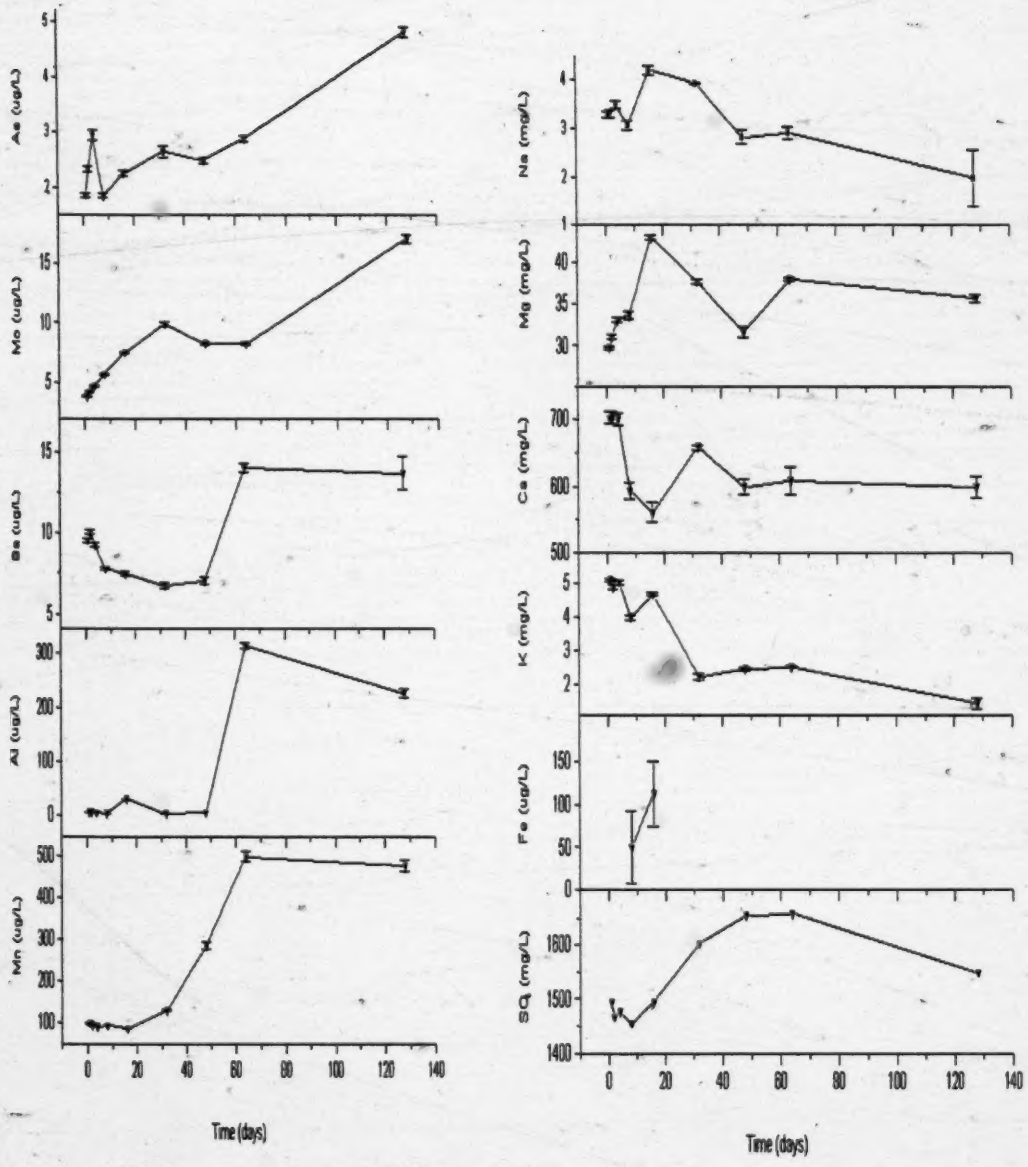

Figure 11. Mean concentrations (with errors) of major (Na, Mg, Ca, K, Fe, and SO_4) and minor (As, Mo, Ba, Al, and Mn) solution ions in the pore water samples extracted from the shale/till plotted against number of days since the start of the equilibration.

Na, K, and SO_4 ions are still fluctuating at the end of the equilibration indicating a system not in equilibrium. Solution arsenic concentration changes data supports the conclusion that the system is not in equilibrium. The increasing trend in arsenic (and Mo) at the end of the equilibration is opposite to all other solution ions which are either stable or decreasing in concentration. The change in Mo concentration closely mirrors any changes in As concentration over the latter part of the equilibration. As mentioned previously a strong relationship in the adsorption and desorption behavior between aqueous arsenic and molybdenum has been reported by Alberta Health and Wellness (2000). Due to the fact that As and Mo are reacting in the same way in the shale/till equilibration and because of the previously stated relationship, it is possible that adsorption/desorption reactions are controlling both ions. If precipitation is controlling aqueous arsenic concentrations, there should be a solution cation that displays a similar trend in concentration changes over the equilibration. This was not seen in the data, and in fact the trend in concentration changes for all solution cations display an opposite trend (decreasing concentration) at the end of the 4-months compared to arsenic. The release of iron and formation of iron oxides after the breakdown of jarosite was not observed in the shale/till equilibration. Jarosite can persist in soil and soil solutions with a pH > 4.0 for decades (Van Breeman, 1982).

The concentrations of solution ions in the shale and shale/till equilibrations are very similar. All ion concentrations do not differ by more than an order of magnitude with the exception of Al and Fe ions. The concentration of Al is over 2 orders of magnitude higher in the shale equilibration and Fe was as much as 3 orders of magnitude higher in the shale system. Aluminum solubility is pH dependent with crystalline and amorphous Al compounds increasing in solubility as the pH decreases below pH 5.5. The minimum solubility for iron and all of its crystalline and amorphous solid compounds is in the 7.4 to 8.5 pH range with increasing solubility the further pH moves away from this range. This would explain why there is more solution Al and Fe in the shale equilibration.

3.3 Activity Ratio Diagrams

Activity ratio diagrams were constructed to assess the process or mechanism (adsorption or precipitation) responsible for limiting aqueous phase arsenic concentrations in both the shale and shale/till experiments. These diagrams were specifically constructed for both the shale and shale/till systems. Two diagrams were constructed for each system, the first representing the 4-month equilibration assuming non-equilibrium conditions and the second representing the system at infinite time assuming equilibrium. The equilibrium reactions needed in the construction of the activity ratio diagrams were taken from Lindsay (1979) and Sadiq (1997). All reactions assume a temperature of 25 °C and 1 atmosphere of pressure.

3.3.1 pH/pE diagrams

The first step in constructing the activity ratio diagrams is determining the solution species of arsenic. The equilibrium reactions used are specific to one solution ion species. These solution ions will change depending on the pH and the Eh (redox) of the system under study. The pE used in the pH/pE diagrams is simply the measured Eh probe value (in mV) divided by 59.2. The pE value expresses the redox status of the system under study as the –log of electron activity, similar to the way pH is expressed. This allows for easier comparison of the 2 parameters. The completed pH/pE diagrams for the shale and shale/till experiments can be seen in Figure 12 and Figure 13. The stability fields of the various aqueous arsenic species are illustrated on the diagrams. Activities (calculated from the aqueous concentrations) of arsenic and sulfate measured during the 2 experiments were used in the construction of the 2 diagrams. The resulting diagrams are specific to either the shale or the shale/till systems under study. A pH/pE point measured at each of the 9 time periods during the shale or shale/till equilibration is plotted on the graphs. Figure 12 and Figure 13 indicate that the likely solution species of arsenic in both the shale and shale/till equilibration is $H_2AsO_4^-$.

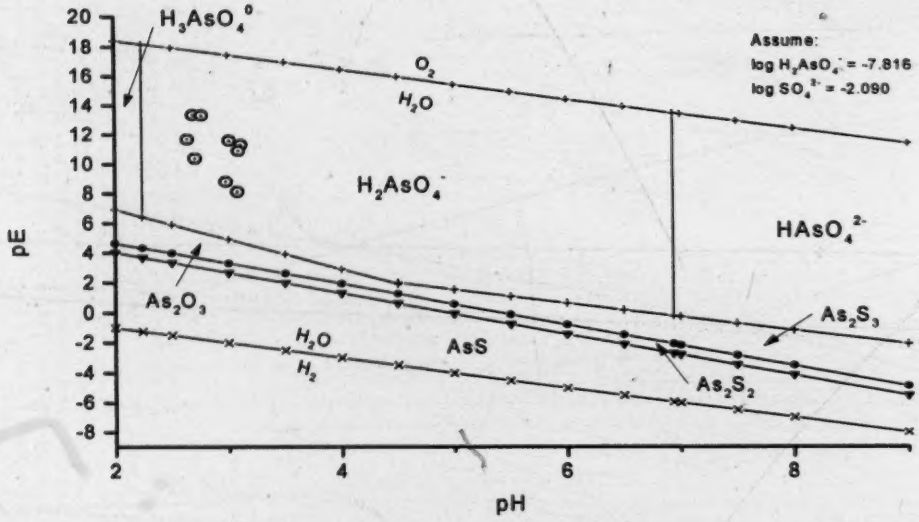

Figure 12. Eh-pH Diagram for the As-S-O-H system illustrating the most likely solution species of arsenic in the shale system. The pH/pE point measured at each of the 9 equilibration times is plotted on the graph

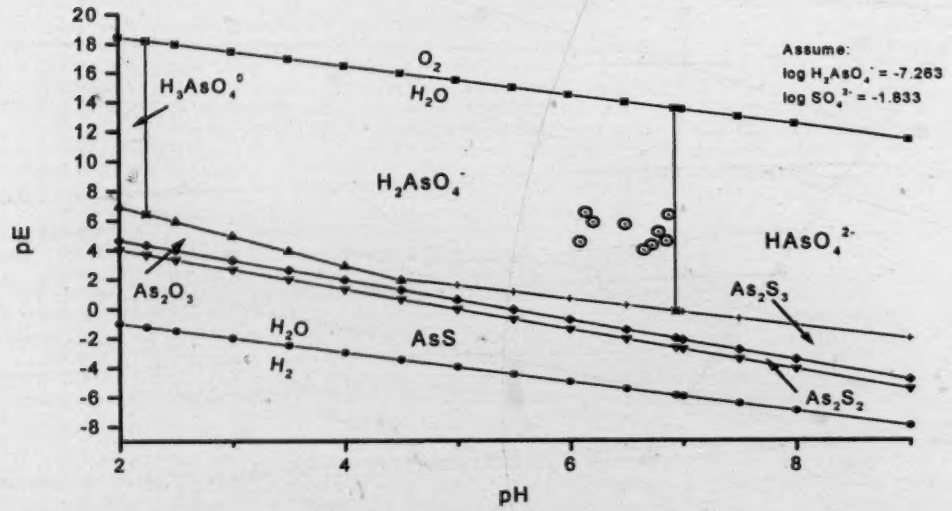

Figure 13. Eh-pH Diagram for the As-S-O-H system illustrating the most likely solution species of arsenic in the shale/till system. The pH/pE point measured at each of the 9 equilibration times is plotted on the graph.

3.3.2 Conversion of equilibrium reactions used in the construction of activity ratio diagrams (ARD)

All of the thermodynamic equilibrium reactions for the possible metal-arsenate precipitates were taken from Sadiq (1997). These reactions and the corresponding equilibrium constants are specific to the $HAsO_4^{2-}$ solution species of arsenic, which is common in the pH range of 7 to 11 in oxidized environments. Deriving the equilibrium reactions specific to the $H_2AsO_4^-$ solution arsenic species predicted in the previous section in both the shale and shale/till systems from the pH/pE diagrams involves combining equilibrium equations. An example for iron-arsenate:

$$FeAsO_4(s) + H^+ \Leftrightarrow Fe^{+3} + HAsO_4^{-2} \qquad \log K = -9.45$$
$$HAsO_4^{-2} + H^+ \Leftrightarrow H_2AsO_4^- \qquad \log K = 6.94$$

$$FeAsO_4 + 2H^+ \Leftrightarrow Fe^{+3} + H_2AsO_4^- \qquad \log K = -2.51$$

This final equation can now be used in the construction of an activity ratio diagram specific to the shale and shale/till systems.

3.3.3 Activity ratio diagrams: non-equilibrium

Activity ratio diagrams specific to either the shale or shale/till system over the 4-month equilibration were constructed assuming a state of non-equilibrium. The diagrams were constructed using measured ion concentration data recorded during the shale and shale/till equilibration experiments. The technique used in the construction of the diagrams was adapted from Lindsay (1979). Initially the equilibrium reactions for the various metal-arsenate compounds, taken from Sadiq (1997), are manipulated to yield a relationship between the activity of aqueous arsenic as it varies with pH.

A summary of the method follows:

$$a\,(\text{metal-arsenate precipitate}) + x\,(H^+) \Leftrightarrow b\,(\text{aqueous metal ion}) + c\,(\text{aqueous arsenate}) = K$$

where:

$$K = \frac{(\text{aqueous metal ion})^b\ (\text{aqueous arsenate})^c}{(\text{metal-arsenate precipitate})^a\ (H^+)^x}$$

Taking the log of both sides:

Log K = b log (aqueous metal ion) + c log (aqueous arsenate) - a log (metal-arsenate precipitate) - x log (H^+)

-then: - the activity of a solid is 1 and the log 1 = 0

- and the –log of (H^+) = pH

-the final equation:

c log (aqueous arsenate) = - x pH + log K – b log (aqueous metal ion)

An example calculation using calcium as the metal and using the measured Ca concentration (and resulting activity) determined during the shale equilibration:

Calcium.

$$Ca_3(AsO_4)_2(s) + 4H^+ \Leftrightarrow 3Ca^{+2} + 2H_2AsO_4^- \qquad \log K = 11.97$$

$$\log K = 3\log(Ca^{+2}) + 2\log(H_2AsO_4^-) - 4\log H^+ - \log(Ca_3(AsO_4)_2)$$

where $\log(Ca^{+2}) = -2.257$ (measured during the shale equilibration)

and $\log(Ca_3(AsO_4)_2) = 0$

$$2\log(H_2AsO_4^-) = -3(-2.257) - 4pH + 11.97$$

$$\log(H_2AsO_4^-) = 9.37 - 2pH$$

This last equation is used to graph the calcium arsenate equilibrium line on the shale activity ratio diagram specific to the 4-month equilibration assuming non-equilibrium. These equilibrium lines will shift up or down depending on the cation activity. Equilibrium lines were constructed using the measured concentrations (and resulting activities) for the least soluble metal-arsenate compounds in the shale and shale/till systems. The result is an activity ratio diagram specific to the shale system over the 4-month equilibration assuming a state of non-equilibrium. The metal ion activities used in the construction of the diagrams was an average over the 4-month

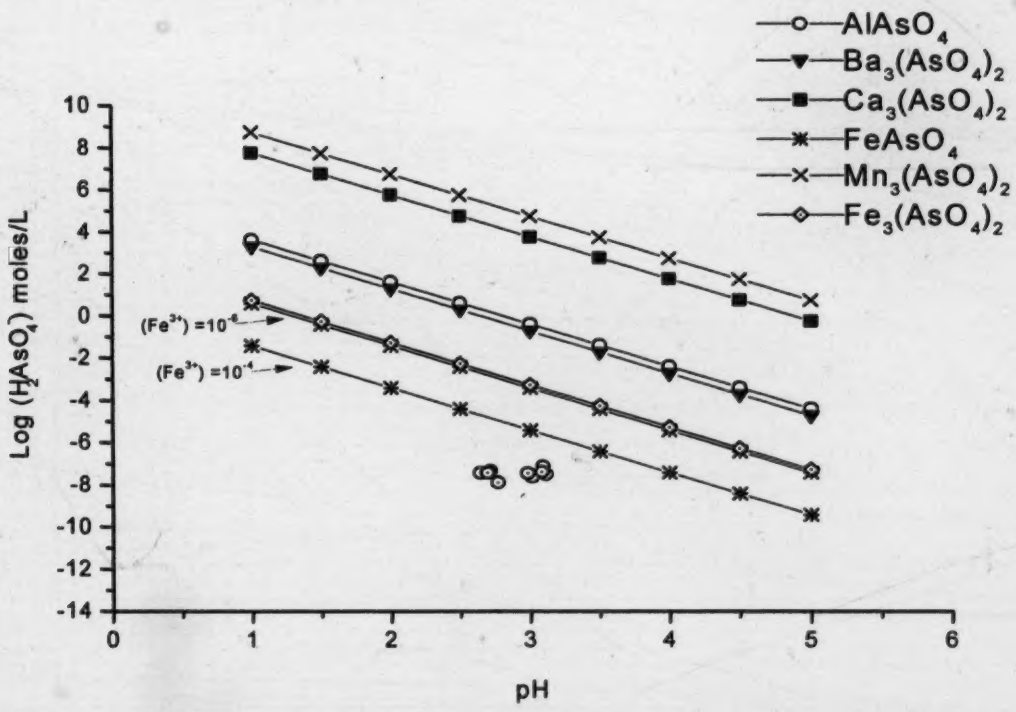

Figure 14. Activity ratio diagram outlining possible metal-arsenate precipitates in the shale system over the 4-month equilibration assuming non-equilibrium. Actual measured arsenic concentrations (activities) for each of the 9 equilibration times are plotted on the graph.

equilibration. Using the maximum and minimum metal ions activities over the 4-months will shift the lines but this shift was small enough that only the average was used in this presentation. This small shift was due to the relatively small change in all metal ion activity over the 4-months. The one exception was the large shift in iron activity in the shale equilibration (421 mg/L change). In this case, 2 separate equilibrium lines were constructed using the maximum and minimum activity over the 4 months. The resulting equilibrium lines are far enough apart to necessitate

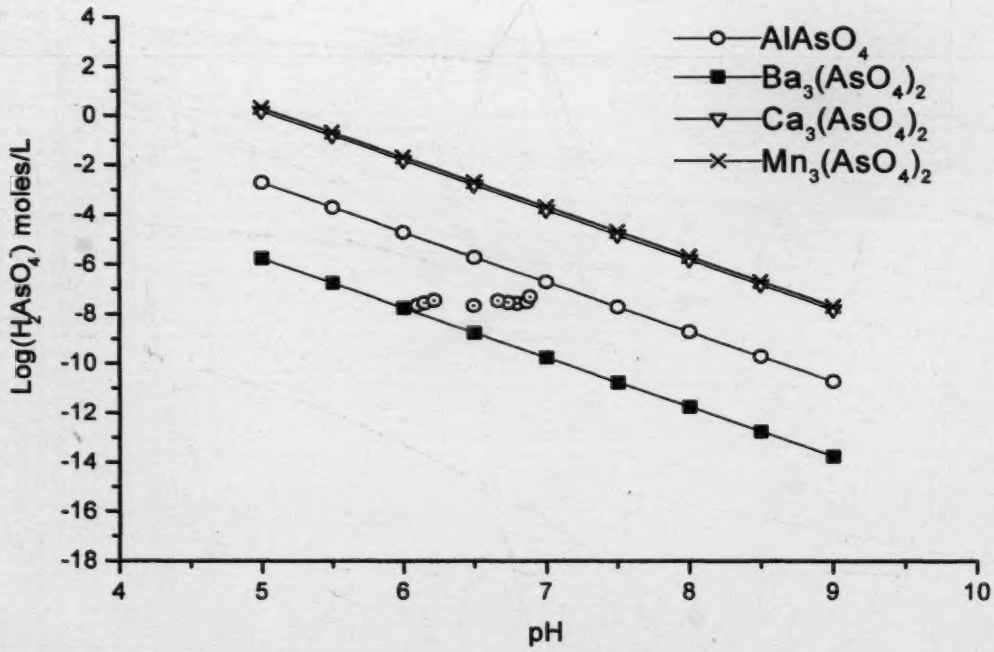

Figure 15. Activity ratio diagram outlining possible metal-arsenate precipitates in the shale/till system over the 4-month equilibration assuming non-equilibrium. The actual measured arsenic concentrations (activities) for each of the 9 equilibration times are plotted on the graph.

plotting both in the activity ratio diagram (ARD). The activity ratio diagrams for the shale and shale/till equilibrations over the 4-month equilibration assuming non-equilibrium is presented in Figures 14 and 15. Points on the ARD represent an ion activity (arsenic in this case) measured during one of the 9 equilibration periods. If the point is on or close to one of the lines, it suggests equilibrium between the solution ion species and the solid precipitate that the line represents and the interpretation is the solid phase is present and controls the solution ion concentration of arsenic. Points above the line indicate a system that is over-saturated with respect to the solution species of the ion. In this case the precipitation of the least soluble solid will occur until the solution concentration is reduced to a point that falls back down to the equilibrium line representing a state of equilibrium. The lower the line the less soluble the precipitate is. This lowest line (and the precipitate it represents) normally forms before all others and sets the equilibrium solution ion concentration. This rule can change due to kinetics and other factors. Points below all equilibrium lines represents a system that is under-saturated with respect to the ion under study and indicates that:

- a process other than precipitation is responsible for limiting the aqueous phase ion concentration; or
- there is a yet undiscovered precipitate (and line) that is limiting the aqueous ion concentrations; or
- the current thermodynamic data used in constructing the activity ratio diagram is incorrect.

In the shale system (Figure 14), the 9 aqueous arsenic activity points all fall below the equilibrium lines indicating a state of under saturation for all 9 equilibration times. In the shale/till system (Figure 15), the 9 points representing aqueous arsenic activity falls on (initially) or above the barium-arsenate line. This indicates a system that is at equilibrium or over saturated. These diagrams will be discussed later.

An activity ratio diagram was constructed to illustrate the equilibrium relationship between solution iron and possible precipitated iron oxides in the shale equilibration experiment (Figure 16). The diagram illustrates the flood of solution iron after jarosite breakdown, moving the system away from equilibrium, and the

subsequent precipitation of ferrihydrite to restore solution iron equilibrium (Figure 16). In Figure 16, the solution iron concentrations (activities) for each of the 9 time periods over the equilibration is illustrated. The pH in the shale equilibration steadily increases up until the end of the 4-months, meaning the further left points represent the earlier time periods in the equilibration. Referring to Figure 16, starting roughly from left to right (start of equilibration to the end), the 3 points (days 1, 2, and 4) on the line (inverted triangles) represent the state of equilibrium before the jarosite breakdown. Then the 3 points above the line (diamonds)(days 8, 16, and 32) indicate a state of over-saturation of solution iron due to the breakdown of the jarosite mineral

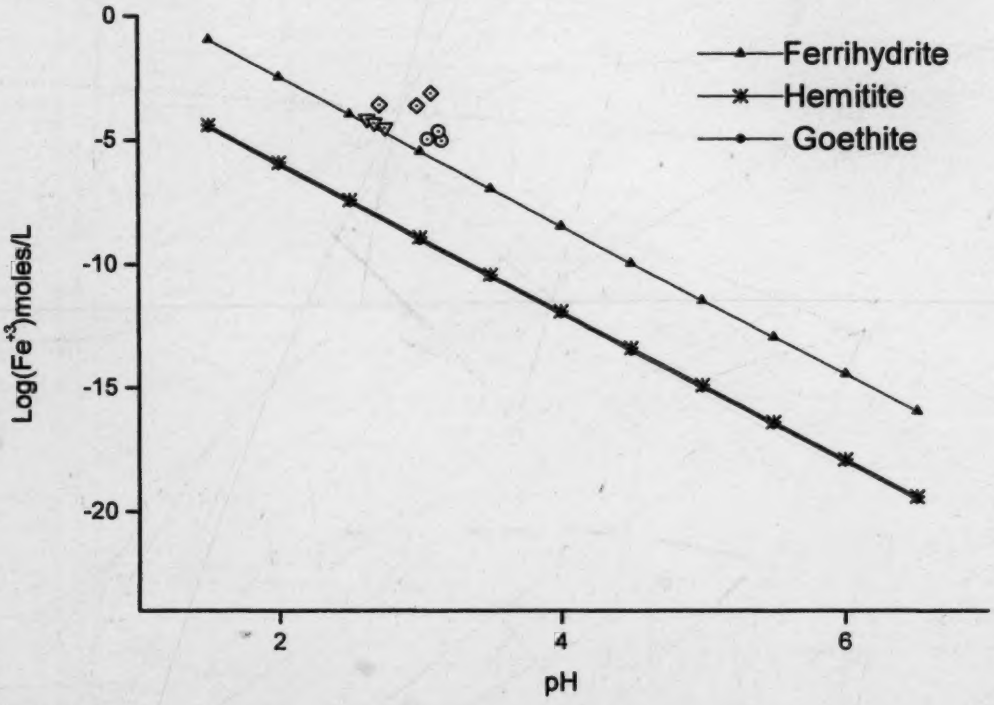

Figure 16. Activity ratio diagram outlining possible iron oxide precipitate formation in the shale system. Actual measured iron concentrations (activities) are plotted on the graph for each of the 9 equilibration times.

and the release of the iron into solution followed by the precipitation of ferrihydrite. The last 3 points (days 48, 64, and 128)(circles) drops back near the line, indicating a drop in solution iron due to the ferrihydrite formation and a return to a near equilibrium state. Figure 16 illustrates one of the cases where the equilibrium ion concentration is not controlled by the lowest equilibrium line. There are 2 reasons why this occurs:

- the extreme oxidation of this system due to the low pH and unlimited access to atmospheric oxygen;
- the large amounts of solution silicon resulting from the high acidity and large clay content of the shale.

Both of these factors result in the preferential formation of ferrihydrite (Schwertmann et al., 1989). In addition, reaction kinetics favors the formation of ferrihydrite, which reverts to goethite with aging over time.

3.3.4 Activity ratio diagrams-equilibrium

Activity ratio diagrams were also constructed for the shale and shale/till systems assuming equilibrium. These diagrams do not apply to the non-equilibrium 4-month equilibration period but represents these systems after all solution ions have reached a state of equilibrium. At equilibrium, all of the solution metal ions that are most likely to form precipitates with arsenic will be in equilibrium with some compound (solid) and this compound will control or limit the aqueous concentrations of this ion. For example, the solution concentration of iron will be dictated by iron oxide formation and calcium solution concentrations will be controlled by gypsum. These equilibrium activity ratio diagrams do not use measured ion activities in the formation of the equilibrium lines. A manipulation of the solubility formula controlling metal ion concentrations yields a constant that varies with pH which is then inserted into the metal-arsenate equation in place of the measured metal activity. The result is a general equilibrium line and resulting activity ratio diagram that is applicable to any system that is in equilibrium. An example of this procedure for iron:

Reaction for amorphous iron oxide (quickest and most likely in soil systems) which controls aqueous iron after equilibrium has been reached:

$Fe(OH)_3 + 3H^+ \Leftrightarrow Fe^{+3} + 3H_2O \qquad log\ K = 2.70$

-manipulating the equation to isolate Fe^{+3}

$\log K = \log(Fe^{+3}) + 3\log H_2O - \log Fe(OH)_3 - 3\log(H^+)$

-where: $\log (H_2O) = 0$ and $\log (Fe(OH)_3) = 0$

$\log(Fe^{+3}) = 2.70 - 3pH$

-now using this 2.70 – 3pH in the original iron-arsenate equation instead of the actual measured iron activity:

$FeAsO_4 + 2H^+ \Leftrightarrow Fe^{+3} + H_2AsO_4^- \qquad \log K = -2.51$

$\log K = \log(Fe^{+3}) + \log(HAsO_4^-) - 2\log(H^+) - \log(FeAsO_4)$

$\log K = \mathbf{2.70} - \mathbf{3pH} + \log(H_2AsO_4^-) - 2\log H^+ - \log(FeAsO_4)$

$\log(H_2AsO_4^-) = -5.21 + pH$

This equation represents the equilibrium line for iron-arsenate in a system assumed to be in equilibrium when the concentration of solution iron is controlled by iron-oxide formation. This technique was used to derive equilibrium solubility lines for all the ions likely to form metal-arsenate precipitates. Figure 17 illustrates the activity ratio diagram for the shale system at equilibrium. The activity of arsenic at equilibrium was determined from data in Figure 7. The compounds in equilibrium with and controlling metal solution ion concentrations are displayed in Figure 17 (for example Al is in equilibrium with $Al(OH)_3$). Figure 17 indicates that the shale system is under saturated with respect to solution arsenic when the system reaches a state of equilibrium. This will be discussed later.

Figure 18 illustrates the activity ratio diagram for the shale/till system at equilibrium. The concentration (activity) of arsenic at equilibrium (infinite time) was determined from data in Figure 8.

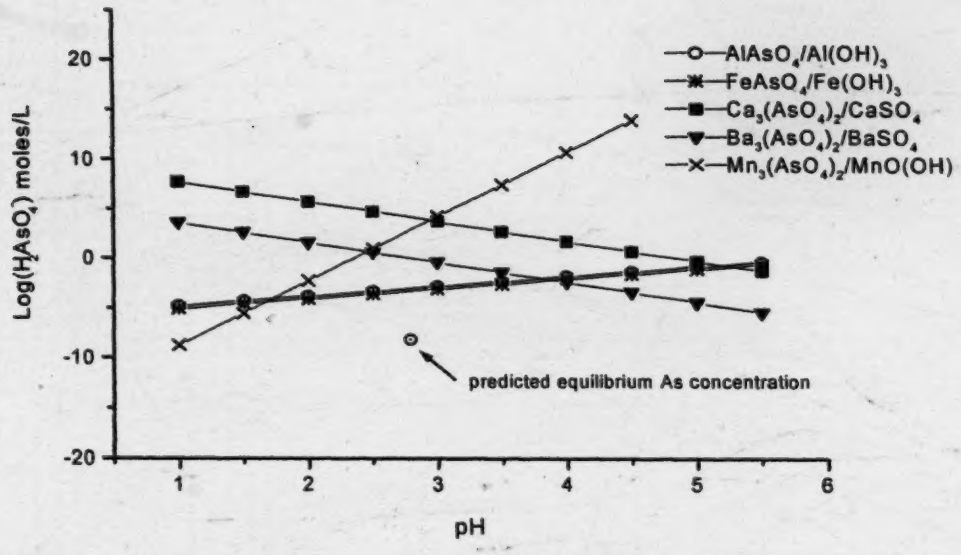

Figure 17. Activity ratio diagram for the shale system at equilibrium (infinite time). The predicted equilibrium arsenic activity is plotted on the graph.

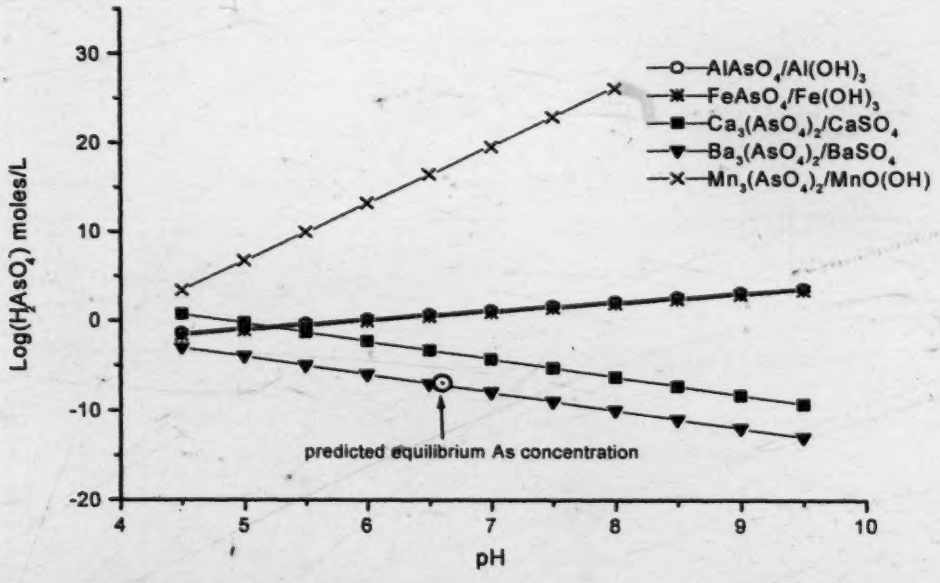

Figure 18. Activity ratio diagram for the shale/till system at equilibrium (infinite time). The predicted equilibrium arsenic activity is plotted on the graph

Figure 18 indicates that when equilibrium is achieved in the shale/till system, solution arsenic concentrations are in equilibrium with $Ba_3(AsO_4)_2$.

3.4 Spiking experiment 1

The first spiking experiments were conducted to test experimentally if the theoretical predictions made previously using activity ratio diagrams about the mechanism (adsorption or precipitation) limiting aqueous arsenic is correct. Three different concentrations (4, 25, and 100 μg/L) of arsenic were added to the solution portion of the samples removed after centrifugation. Shale samples were equilibrated for 7 days, the solution portions of the samples were removed, and the arsenic spikes were added to the removed solution portion of the samples. Shale/till samples were equilibrated for 16 days, followed by the removal of the solution portion of the samples, followed by arsenic spiking. After the arsenic spikes were added, all samples were equilibrated for another 8 days and then analyzed for solution cation and anion concentrations.

Figure 19 shows the results of the spiking experiment on the solution portion of the marine shale experiment. The *before* arsenic concentration represents the arsenic spike (either 4, 25, 100 μg/L) and any natural background arsenic present in the soil solution. The *after* arsenic concentration represents the total amount of arsenic in the solution after the spiking and 8 days of further equilibration.

Figure 20 shows the results of the spiking experiment in the shale/till mixture.

3.5 Spiking experiment 2

The second spiking experiment was conducted to determine if metal-arsenate precipitates would form if the concentration of solution arsenic was high enough. Any precipitate formed will be compared to precipitates predicted by the activity ratio diagrams. A large concentration or spike of arsenic was added (0.1 mol/L) to the removed solution portion of the shale and shale/till samples. The spiked samples

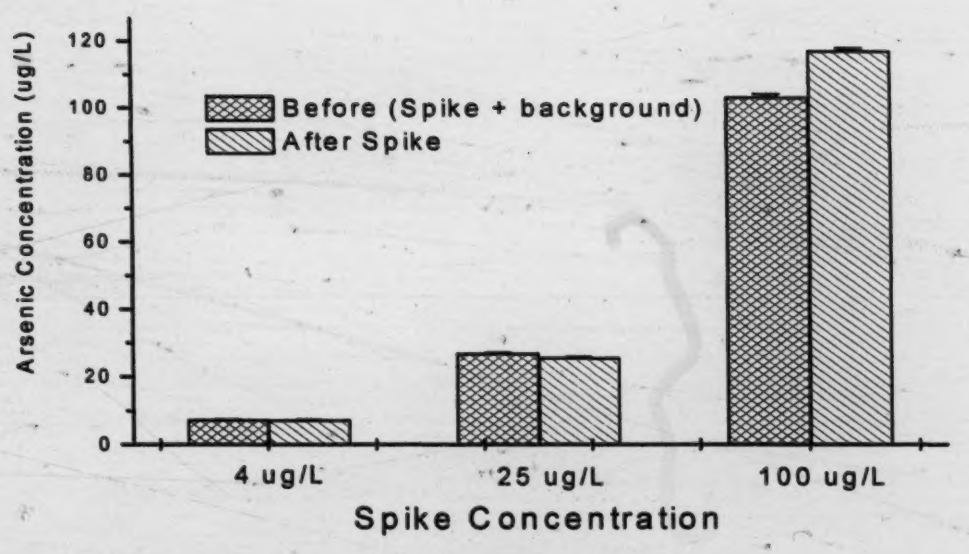

Figure 19. Concentration of solution arsenic in the shale system before (which includes the arsenic spike concentration and any natural background arsenic) and the concentration of solution arsenic after the spike.

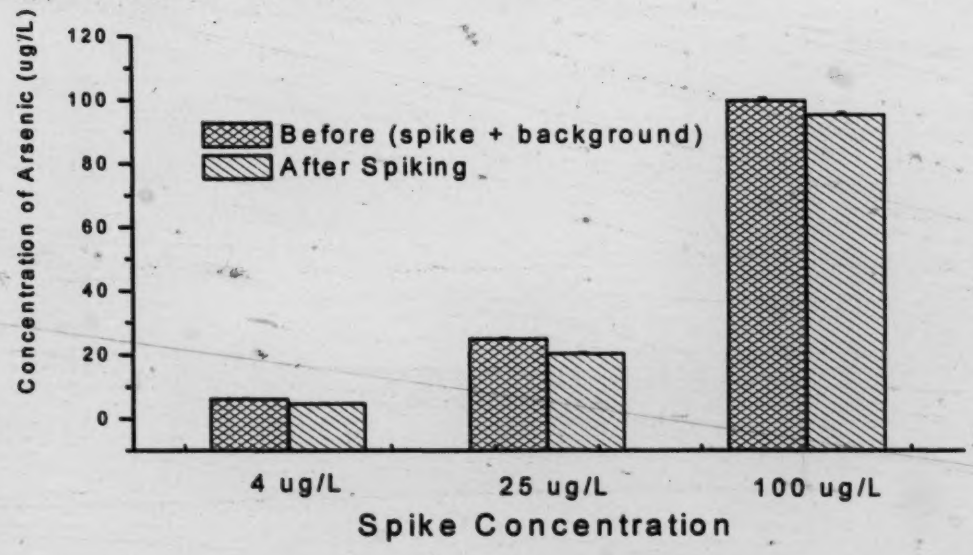

Figure 20. Concentration of solution arsenic in the shale/till system before (which includes the arsenic spike concentration and any natural background arsenic) and the concentration of solution arsenic after the spike.

were allowed to react for another 8 days before solution cation and anion concentrations were determined. The concentrations of the major cations in solution before and after the spike for the shale and shale/till systems are presented in Appendix 2. The concentration and resulting activity of arsenic before and after the spike in the shale system is illustrated in Figure 21.

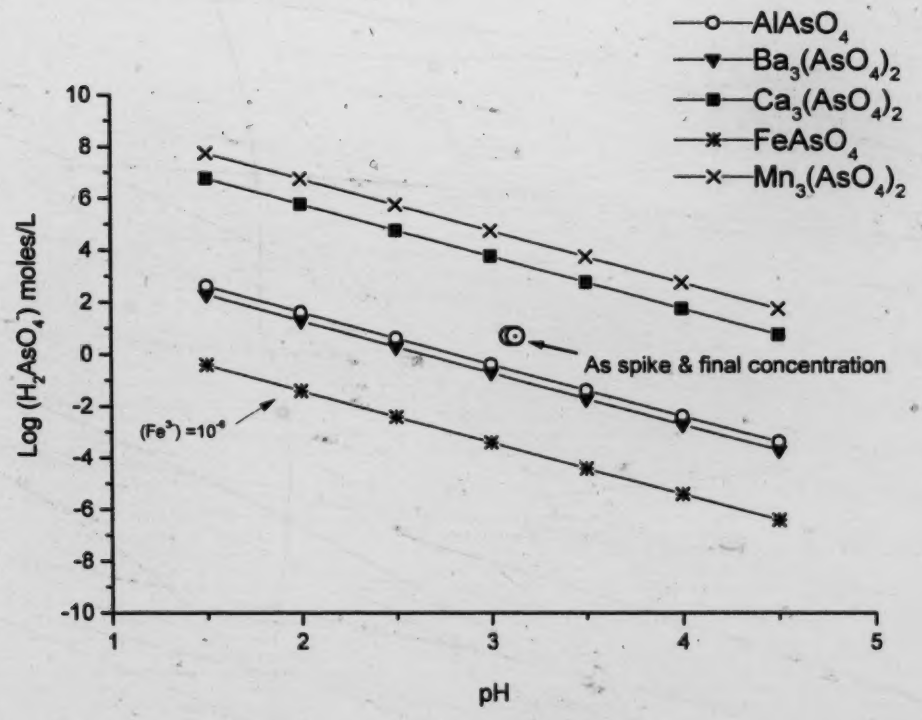

Figure 21. Activity ratio diagram for the shale system outlining the measured arsenic concentration (activity) before (which includes the arsenic spike concentration and any natural background arsenic) and arsenic activity after the spike and any possible precipitation reactions.

The 2 points plotted on the ARD (looks like one point) represents the activity of arsenic before (which includes the spike concentration and any solution arsenic

present naturally) and after the 8 days of further reaction time. It appears that only one point is plotted because the activity of arsenic and the pH of the system did not change enough to separate the points. A white precipitate did form approximately 30 sec after the arsenic spike was added. This precipitate was removed, dried, and saved for analysis by XRD and EDX spectral analysis. XRD analysis indicated the precipitate was amorphous. EDX spectral analysis indicated that the compound was a coprecipitated mixed solid that contains approximately 53% As, 1% Fe, 17% Ca, 1% S, 19% Al, and 7% Na. There was a drop in the concentration of the main constituents of this mixed solid, Ca and Al, as seen in Appendix 2. The concentration of Fe also dropped after the spike.

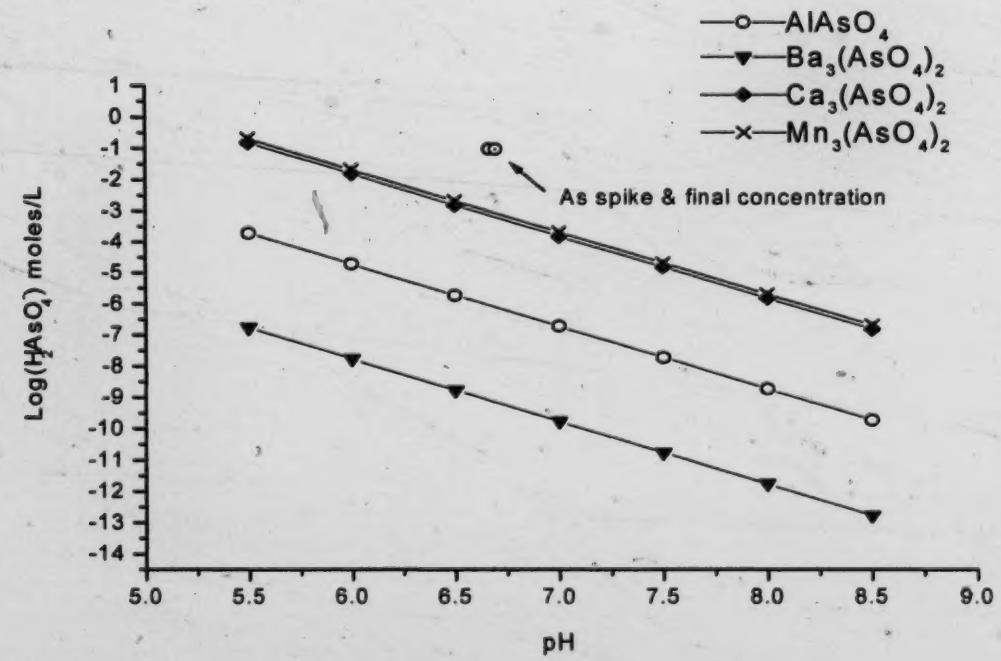

Figure 22. Activity ratio diagram for the shale/till system outlining the measured arsenic concentration (activity) before (which includes the arsenic spike concentration and any natural background arsenic) and arsenic activity after the spike and any possible precipitation reactions.

The activity of arsenic before and after the spike in the shale/till system is illustrated in Figure 22. There are 2 points plotted on the diagram (looks like one point) representing the activity of arsenic before (which includes the spike concentration and any solution arsenic present naturally) and after the 8 days of further reaction time. After the arsenic spike was added, no visible precipitate formed during the 8 day post spike reaction period. Only the concentration of Ca dropped over the 8 day post spike equilibration, but the drop was 3X less than in the previous shale spiking system. Solution arsenic concentrations as high as 0.1 mol/L did not result in any precipitation.

3.6 Spiking experiment 3

In this experiment, shale was initially equilibrated for 16 days to maximize solution iron. The solution portion of these samples was removed and spiked with either 26.4, 100, or 3380 µg/L of arsenic. After approximately 6 days ferrihydrite formed on the sides of the sample containers. The amount of solution arsenic adsorbed and removed from solution by the ferrihydrite was determined after another 16 days of reaction time. Table 3 displays how much of the arsenic was removed for each spike concentration.

Table 3. Concentration of solution arsenic (shale samples) and percent removal after adsorption onto ferrihydrite. Arsenic spike [ ] includes the spike and any natural background arsenic.

Arsenic spike [ ] ug/L	Arsenic [ ] after adsorption ug/L	% arsenic removal %
26.41	1.46	94.5
100	11.3	88.7
3380	36.5	98.9

Table 3 shows that at least 88% of all solution arsenic was removed from the shale system through adsorption onto the newly precipitated ferrihydrite iron oxides. The next step was to determine the partition coefficient (Kd) of arsenic adsorption onto

this ferrihydrite. This was done by graphing the relationship between the dissolved arsenic concentration (Cw) in mg/L to the adsorbed arsenic concentration (X) in mg of As/ kg soil (Sheppard et al., 1992). The slope of the line is the partition coefficient Kd in L of arsenic/ kg ferrihydrite. In this case the "soil" is referring to the ferrihydrite iron oxide that precipitated from solution. The results are shown in Figure 23. The calculated partition coefficient is about 101 L of arsenic/ kg of iron oxide.

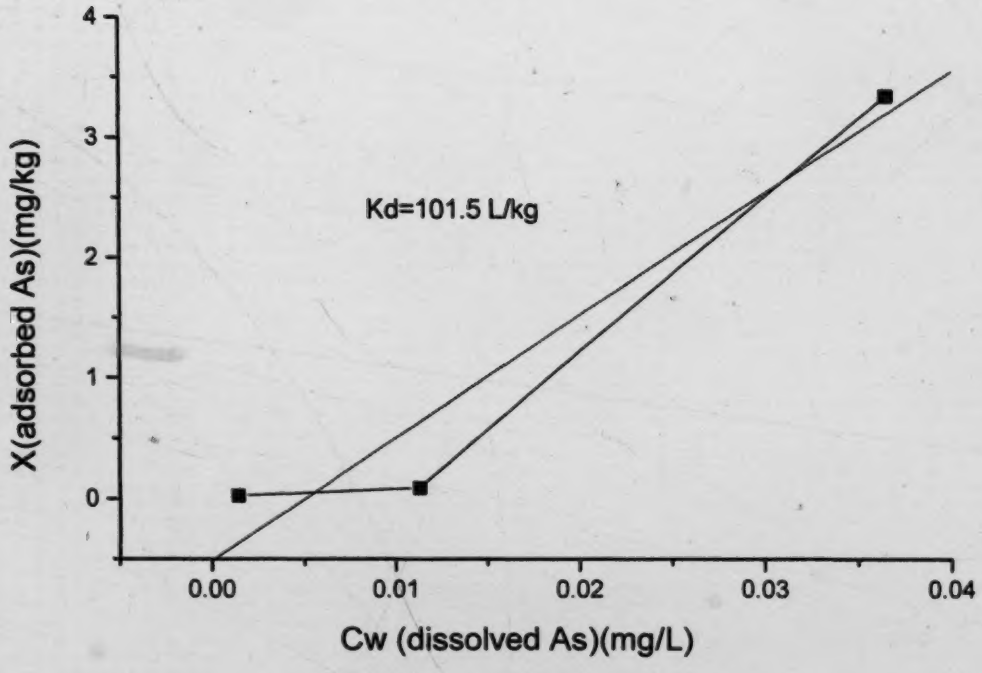

Figure 23. The amount of aqueous solution arsenic (Cw) versus the amount of arsenic adsorbed (X) onto the newly precipitated iron oxides (ferrihydrite). The slope of the line is the partition coefficient (Kd) that represents arsenic adsorption onto the freshly precipitated ferrihydrite in the shale system.

It is also possible to determine the partition coefficient (Kd) of the bulk shale and of the bulk shale/till mixture. This is done using the $t = \infty$ (equilibrium) arsenic concentrations predictions (Figures 7 and 8) from the equilibration experiments. This

equilibrium arsenic concentration value is the Cw value in mg/L. The amount of adsorbed (total) solid phase arsenic or "X" in mg/kg was determined using neutron activation analysis. Dividing the adsorbed concentration (X) by the amount in solution (Cw) yields the Kd value. The Cw at equilibrium or infinite time in the shale is about 0.0006 mg/L and the adsorbed concentration or "X" is about 35 mg As/kg shale. The resulting Kd value for arsenic adsorption in the bulk shale is about 58,000L As/kg shale. The Kd value for arsenic adsorption in the shale/till mixture can be determined in the same way, with a Cw of about 0.01 mg/L and an "X" value of 30 mg As/kg shale/till mixture. The resulting Kd value for arsenic adsorption in the bulk shale/till mixture is about 3000 L/kg.

4.0 Discussion

4.1 Pore water equilibration: marine shale and marine shale and till.

The highly weathered marine shale used in this study contains naturally elevated arsenic concentrations in the 30 mg As/kg shale range. This shale is almost fully oxidized as indicated by the co-existence of jarosite and minute traces of iron sulfides (Mermut et al., 1985). Most of the arsenic in this shale has been released from the host mineral (iron sulfide) and then the element redistributed itself mainly as adsorbed arsenic. Throughout the world, natural arsenic contamination of pore, ground, and surface water released from surrounding marine shale formations is common. In fact, elevated solution arsenic concentrations were expected in this study because of the high concentrations of As in the marine shale and because most of the arsenic had already been released from the original host mineral. However, elevated solution concentrations of arsenic were not found in the experiments. In the 4-month marine shale equilibration, the concentration of solution arsenic reached a maximum of 7 μg/L and the concentration was about 1 μg/L at the end of the 4-month equilibration. This value is well below the 25 μg/L guideline value set out in the Canadian Guidelines for Drinking Water Quality (Health Canada, 1996). The amount of arsenic released from the shale into the solution phase was 10,000X less than the total solid phase arsenic concentration initially found in the shale. The overall trend in solution arsenic concentrations in the shale equilibration was downward (except for the spike at day 4) and the predicted concentration at infinite time (approximation) was between 0.0 μg/L and 0.6 μg/L. It appears that the amount of aqueous arsenic in the boundary soil and its associated parent material will be extremely small (less than 1 μg/L) under constant aerobic conditions. Aqueous phase arsenic contamination should not be an issue. Water samples were taken from 2 surface dugouts near the study area surrounded by the shale material to check if solution arsenic concentrations were low. The amount of aqueous arsenic was determined and found to be 0.08 and 0.6 μg/L. These values seem to back up the claim that the amount of arsenic released from the shale into the surrounding water systems under aerobic conditions is small.

Glacial till (Cca) was added to the shale in the second equilibration experiment. Glacial till was added to increase the pH and any changes to solution arsenic concentrations were determined. Determining and understanding changes to solution arsenic in this mixture is important for two reasons:

a. boundary soils derived from the shale are used for crop production usually with liming amendments to adjust the pH to aid in plant growth; and
b. there are large areas of soils developed on marine shale admixed with calcareous glacial till.

The concentration of solution arsenic in the shale/till equilibration increased especially near the end of the 4-month equilibration. The change in solution arsenic followed the same trend up until day 64 in the shale/till and shale equilibrations. The concentration of arsenic after day 64 increased until the end of the 4-month equilibration in the shale/till mixture unlike the shale only system where the concentration decreased. The addition of till resulted in increased aqueous arsenic concentrations due to the increased pH and additional attendant geochemical reactions of the new mixture. At the end of the 4-month equilibration, the amount of solution arsenic in the shale/till system was 4X greater than in the shale system alone. The concentration of arsenic released from the shale/till mixture once equilibrium has been reached is predicted to be between 5 and 10 μg/L. This value is an estimate and the actual value could be higher than 10 μg/L.

The increase in solution arsenic in the higher pH shale/till mixture is not unexpected because the two main reactions responsible for removing solution arsenic, adsorption and precipitation, are less effective as pH increases. Adsorption and chemisorption onto the various iron oxides/hydroxides is an important mechanism of arsenic removal and has been well documented in the literature. The positive charge of iron oxides/hydroxides that adsorbs the negatively charged arsenic (oxyanion form in solution) diminishes as pH increases. The anion exchange capacity is pH dependent (iron hydroxide/oxides have a Zero Point of Charge when the surface of the oxide has neither a net positive or net negative charge, ranges from 6.5 to 8.0) which results in the shale/till mix having a lower anion exchange capacity than the shale alone. The lower anion exchange capacity in the shale/till mix means less

arsenic adsorption and larger solution arsenic concentrations, which is what was observed in the equilibration experiments. Aluminum hydroxides/oxides can also play a very limited role in adsorbing and removing arsenic from solution. The zero point of charge (ZPC) of aluminum hydroxides/oxides is approximately pH 6. This means that above pH 6 these hydroxides/oxides have a net negative charge and will not adsorb significant amounts of arsenic. The pH in the shale/till mixture is above 6 which eliminates the anion exchange capacity of the aluminum hydroxides/oxides in the shale/till system. Aluminum hydroxides/oxides will remove arsenic in the shale system (about pH 3), but because of the extremely low pH these oxides will begin to breakdown limiting the amount of sorption sites. Amphoteric clays (iron and aluminum oxyhydroxides) in the shale carry a pH-dependent charge. At pH values above the ZPC (as with the shale/till mix), these minerals would have a low anion exchange capacity that results in less adsorption and higher aqueous phase anion ($H_2AsO_4^-$) concentrations. For pH values below the ZPC (the shale system alone) these minerals would have a higher anion exchange capacity which results in increased adsorption and lower aqueous phase anion ($H_2AsO_4^-$) concentrations.

Molybdenum, like arsenic, is another ion that takes on an oxyanion form in solution (MnO_4^{2-}). Molybdenum should act in a similar way to arsenic in solution with respect to anion adsorption on amphoteric clays and iron and aluminum oxides/hydroxides. Changes in the concentration of molybdenum over the 4 months in the shale and shale/till equilibrations closely mirrored changes in arsenic. Equilibration data indicated there is more solution molybdenum in the shale system and less in the shale/till system due to the lower pH in the shale system (compared to the shale/till system) and increased adsorption onto the amphoteric clays and Fe and Al oxides/hydroxides (as mentioned earlier). At the end of the 4 months there was 80X as much molybdenum in the shale/till equilibration solutions compared to the shale system alone.

4.2 Solubility Controls on Arsenic – Adsorption or Precipitation

Understanding the mechanism responsible for controlling and limiting aqueous arsenic concentrations is important to better understand the consequences of elevated arsenic levels (either natural or anthropogenic) in soils and sediments. The mechanism responsible for controlling aqueous arsenic over the 4-month equilibration was determined in two steps. Firstly, activity ratio diagrams were constructed for each system (shale and shale/till) allowing the theoretical prediction of the mechanism controlling aqueous arsenic. These diagrams are used extensively in the soil literature (Lindsay, 1979) to predict if a metal solid (in this case metal-arsenate) phase is controlling the aqueous concentration of the particular ion under study. The diagram is a plot of the log activity [solid/metal] vs. pH and shows the least soluble of the known metal-arsenates solids and the concentration of solution arsenic it can support. Secondly, arsenic spiking experiments were conducted on both systems to test experimentally the previous predictions.

4.2.1 Activity Ratio Diagrams

An activity ratio diagram was constructed representing the shale system over the 4-month equilibration in a non-equilibrium state using measured ion concentration data. This approach identified scorodite ($FeAsO_4$) as the least soluble metal-arsenate solid in the pH range of the shale system (around pH 3). If precipitation controls aqueous arsenic concentrations, scorodite will be the metal-arsenate solid that forms because it has the lowest solubility. Solution arsenic activities for the 9-equilibration times were plotted on the graph. These activities fall well below all the metal-arsenate equilibrium lines indicating that the solution phase of the shale system is under saturated over the 4-month equilibration with respect to known arsenic solid phases. Under saturation means:

a) equilibrium with an arsenic solid phase does not exist, and arsenic solubility and aqueous activity is controlled by adsorption;

b) solubility and aqueous activity of arsenic is controlled by a solid phase that is not identified or known due to a lack of thermodynamic data;

c) solubility is controlled by the least soluble arsenic solid phase ($FeAsO_4$), but the solid phase is not in its normal standard state or the thermodynamic data for this compound ($FeAsO_4$) is in error.

Conclusion (a) is the most likely in this system. Conclusion (b) is possible but unlikely. There has been extensive research on arsenic solid phases and it is unlikely that a major arsenic solid compound has been missed by the numerous studies reported in the soils and environmental literature. Conclusion (c) is possible but unlikely. There have been no reports in the literature of the reduction of activity of metal-arsenate solid precipitates. This reduction of activity has been reported for other ions like cadmium (Bohn, 1983). If the thermodynamic data is in error for scorodite ($FeAsO_4$) it is unlikely the line would drop far enough down to close the considerable gap between the measured arsenic activities and the current scorodite equilibrium line. Conclusion (c) is also unlikely due to the large difference between the lowest equilibrium line corresponding to the least soluble solid (scorodite) and the actual solution arsenic activity. This non-standard state will shift the equilibrium line, but not to such a large degree that the line will drop to the actual solution arsenic activities plotted on the graph. Conclusion (a) is most likely correct, indicating that adsorption and not the precipitation of a solid metal-arsenate compound is controlling solution arsenic concentrations over the 4-month equilibration. This is supported by past research into the solubility and stability of metal-arsenate solids (Dove and Rimstidt, 1985; Robbins, 1981; and Sadiq, 1997). These studies indicate that scorodite is the most likely solid to form in the acidic pH range, but the activity of arsenic in solution has to be in the 0.01 to 0.001 moles/L range in order to form the solid. The $1*10^{-8}$ moles/L arsenic solution activity in the shale system of this study is far below the activity needed for solid formation. The literature indicates that arsenic solid phase precipitation controls solution arsenic concentrations only in contaminated systems with elevated solution arsenic activities, unlike the natural (lower arsenic activity) system of this study. In addition, as pH decreases the amount of arsenic (activity) needed to form any solid phase is increased due to the negative

slope of the equilibrium lines on the activity ratio diagram. All of these factors increase the likelihood that adsorption and not arsenic solid phase precipitation is controlling aqueous arsenic activity. Further, Robbins (1981) indicated that scorodite has a much higher solubility than the thermodynamic data predicts. Dove and Rimstidt (1985) reported that scorodite can form and control solution arsenic from waters draining from arsenic rich ores, but is metastable and will eventually re-release arsenic back into solution. Only one study (Vink, 1996) indicated that scorodite is stable and likely to form under the same Eh, pH, and arsenic activities found in the shale system of this study. Experimental testing was conducted to determine if conclusion (a) or (c) was correct and will be discussed later.

Another activity ratio diagram was constructed representing the shale system at infinite time or at equilibrium. This diagram predicts the solubility reaction that controls aqueous arsenic activity once equilibrium has been achieved. The arsenic activity at infinite time falls well below all metal-arsenate equilibrium lines indicating that the solution phase of the shale system at equilibrium is under saturated with respect to all known arsenic solid phases. It is likely that equilibrium with an arsenic solid phase does not exist, and arsenic solubility and aqueous activity is controlled by adsorption in the shale system at equilibrium. The same prediction was made for the shale system over the 4-month equilibration in a non-equilibrium state. The rationale for this prediction was previously discussed for the non-equilibrium shale systems and is the same for the shale system at equilibrium.

The activity ratio diagram representing the shale/till system in a non-equilibrium state over the 4-month equilibration indicates that barium-arsenate ($Ba(AsO_4)_2$) is the least soluble solid phase and most likely to form if conditions favor precipitation. The arsenic activities for the 9 time periods over the 4-month equilibration (Figure 15) in the shale/till systems are initially close to the equilibrium line for barium-arsenate, but moves away from the line as time and pH increases. At the end of the 4-months, the arsenic activity is much higher than the barium-arsenate equilibrium line and below all other metal-arsenate equilibrium lines. This indicates that the system is over-saturated with respect to aqueous arsenic. Normally, if a system is over-saturated (or the activity of the ion is above the lowest equilibrium

line) precipitation of the least soluble solid (corresponding to the lowest equilibrium line) will occur until the solution activity of the aqueous ion drops down to the lowest line and equilibrium is restored. This does not happen in the shale/till systems over the 4-month equilibration. This means that:

a) solution arsenic is controlled by the least soluble arsenic solid phase barium-arsenate, but the solid phase is not in its normal standard state;
b) the thermodynamic data on barium-arsenate is not accurate and equilibrium with an arsenic solid phase does not exist, and arsenic aqueous activity is controlled by adsorption.

In the shale-till system, conclusion (a) is possible but unlikely. If barium-arsenate is not in its standard state the corresponding equilibrium line can shift up, but it is very unlikely the line would shift far enough up to reach the level of the measured arsenic activities. Conclusion (b) is the most probable, indicating that the current thermodynamic data for barium-arsenate solid precipitates is inaccurate. Sadiq and Alam (1996) stated that there is a lack of reliable thermodynamic data for possible metal-arsenate solids. Arsenic spiking experiments were conducted to prove if barium-arsenate or any other metal-arsenate solid is limiting aqueous arsenic concentrations and is presented in the next section. In addition, the thermodynamic data used in the construction of the activity ratio diagrams has limitations when being applied to soil systems. This data is compiled using "clean" systems. For example, in the case of barium-arsenate, the equilibrium constant or K used in the construction of the equilibrium line in the activity ratio diagram is determined using a system that contains only barium and arsenic. The soil systems used in this study contain many interacting ions. How well this data can be applied to soil systems that contain multiple solution ions each reacting and interacting is unclear. In addition, the thermodynamic data for each solid was compiled at a specific pH. Because of the general linear relationship between log solubility and pH (X and Y axis on the activity ratio diagram) the practice of extrapolating to conditions of higher and lower pH is common. This can lead to errors when assessing precipitate solubilities at other pH values (Robins, 1981).

The activity ratio diagram representing the shale/till system at equilibrium (infinite time) indicates that aqueous arsenic is in equilibrium with barium-arsenate. This implicates barium-arsenate as the solubility controlling solid. The activity of aqueous arsenic falls on the equilibrium line for barium-arsenate. However, it is possible and likely that adsorption and not precipitation of a barium-arsenate solid controls solution arsenic in the shale/till systems at equilibrium. The reason for this conclusion is the flawed thermodynamic data for barium-arsenate as mentioned previously for the shale/till systems in a non-equilibrium state. Because these predictions apply to the shale/till system at infinite time or at equilibrium, it is impossible to test experimentally this prediction with arsenic spiking experiments due to the amount of time that would be needed to obtain a complete data set.

4.2.2 Arsenic Spiking Experiment 1

Arsenic spiking experiment 1 was conducted to test experimentally if a metal-arsenate solid phase is controlling aqueous arsenic concentrations. After spiking the final aqueous phase arsenic concentrations will be the indicator of whether a solid phase controls solution arsenic concentrations. Spiking was done on the removed solution portion of the samples to eliminate any possible adsorption to the shale and/or till solid phases that would interfere with the formation of an arsenic solid phase precipitate. If the concentration of arsenic after spiking does not converge or drop down to the same concentration, then chemical precipitation does not exert a control on aqueous phase arsenic concentrations. This final concentration (or activity) would represent a point on the lowest equilibrium line for the least soluble metal-arsenate precipitate in equilibrium with aqueous arsenic restoring a state of equilibrium in the system.

No drop in arsenic concentration was observed after spiking in the shale system indicating chemical precipitation does not control aqueous arsenic concentration over the 4-month equilibration before the system has reached equilibrium. This confirms the theoretical conclusion (from the activity ratio diagram) that equilibrium with an arsenic solid phase does not exist and arsenic

solubility and aqueous activity is likely controlled by adsorption. This is consistent with the literature that states adsorption onto iron oxides/hydroxides is the dominant force removing aqueous arsenic in systems with solution arsenic concentrations of less than 0.01 moles/L.

No uniform drop in arsenic concentration was observed after spiking in the shale/till mixture indicating chemical precipitation does not control aqueous arsenic concentrations. The theoretical prediction from the shale/till activity ratio diagram indicated there was a possibility that barium-arsenate controls aqueous arsenic concentration. This spiking experiment proves that chemical precipitation of barium-arsenate does not control aqueous arsenic concentrations. It is likely that adsorption controls aqueous arsenic concentrations in the shale/till system over the 4-month equilibration before the system has reached equilibrium.

4.2.3 Spiking Experiment 2- Super Saturation

The following spiking experiment was designed to determine if solid phase precipitation would control and limit aqueous arsenic concentrations if the concentration of arsenic in solution was well in excess of the concentration maintained by known solubility controlling solid compounds. Past studies have reported that solid phase precipitation in arsenic contaminated soil systems controls aqueous arsenic concentrations (Dove and Rimstidt, 1985; Vink, 1996). An arsenic spike of 0.1 moles/L was added to the removed solution portion of the shale and shale/till systems. This results in an arsenic activity well above the lowest equilibrium line in both systems. Theory predicts that the least soluble solid phase arsenic precipitate should form (the solid represented by the lowest equilibrium line) dropping the aqueous arsenic activities down to the lowest equilibrium line and restoring equilibrium in the system.

In the shale system, a white precipitate did form from solution within a minute after super saturation spiking. The activity of solution arsenic did fall (slightly) but not down to one of the lower equilibrium lines. The precipitate was amorphous and contained arsenic, calcium, aluminum, and traces of iron. This is not the iron-

arsenate (scorodite) predicted from the activity ratio diagram. The solid produced is a mixture formed from a coprecipitation reaction (Sposito, 1981). These solids have not been extensively studied (Vaslow and Boyd, 1952; Davies and Natrotsky, 1983) and are poorly understood due to the complexity of the reactions involved. Certain coprecipitation reactions also involve adsorption and might better describe the reaction that occurred to form the mixed solid in the shale system. If free diffusion is not possible during precipitation, ions (cations or anions) may still coprecipitate by adsorption. Examples of this process have been reported for iron and aluminum precipitation. During formation, other solution cations and anions will adsorb on the surface of the precipitate. These ions cannot diffuse into the bulk solid, preventing the formation of a true solid solution (Sposito, 1981) accounting for the amorphous nature of the precipitate. The conditions of rapid precipitation and pronounced supersaturation of this spiking experiment favors this type of coprecipitation (Sposito, 1981). A recent study by Sadiq and Alam (1996) proposed a similar theory for arsenic interactions in groundwater/soil systems. This theory combines both solid phase formation and adsorption, similar to the coprecipitation/adsorption theory above.

There were no solid phase precipitates formed after supersaturation spiking from the solution portion of the shale/till system. Activity ratio diagrams predicted that arsenic solution concentrations were high enough to support the precipitation of barium, calcium, or manganese arsenate from solution. This did not happen.

Activity ratio diagrams constructed from the latest thermodynamic data used for predicting solid phase arsenic precipitation from natural or elevated arsenic soil systems appears to be an unreliable approach. This is most likely due to the complexity of soil solutions and for reasons outlined in section 4.2.1.

4.2.4 Spiking Experiment 3 – Partition Coefficient (Kd)

A spiking experiment was conducted to determine the partition coefficient (Kd) for arsenic adsorption on to freshly formed ferrihydrite iron oxide fraction of the marine shale. The partition coefficient is calculated by dividing the amount of the ion under

study adsorbed by the amount of that ion remaining in solution. Three different concentrations of arsenic (spike) were added to the removed solution portion of the shale after equilibration. The concentration of solution arsenic was determined before and after adsorption onto the ferrihydrite iron oxides that had formed on the sides of the sample containers. Partition coefficients are useful in modeling the fate and behavior of contaminants in soil. Modeling contaminant movement over longer times, decades or centuries, using partition coefficients (Kd) for both organic and inorganic contaminants is adequate (Sheppard and Thibault, 1990; Sims, 1990).

A partition coefficient (Kd) specific to the soil (shale) system under study is essential to generate accurate predictions of contaminant (arsenic) movement. A few examples of current models requiring Kd values as input parameters that have undergone partial validation are (Sheppard et al., 1992): SCEMR, EXSOL, SGELG, and CREAMS. A value of 101.5 L As/kg iron oxide was determined in this study which seems reasonable when compared to values found in the literature. Manning and Goldberg (1997) determined the Kd value of an iron-rich Californian soil to be 100 L As/kg of soil. Sheppard and Thibault (1990) determined a generalized Kd value for arsenic soil adsorption of 200 L As/kg soil. There are large differences in soil Kd values due to the variability in soil properties, pH, and test method differences. The Kd of 101.5 L/kg represents arsenic adsorption onto the freshly precipitated iron oxide fraction and not the Kd of the bulk shale. Estimates of the Kd values for the bulk shale and shale/till systems were also determined by dividing the total solid phase arsenic concentration or X by the concentration of arsenic in the solution phase or Cw. A Kd value of approximately 58,000 L/kg was calculated for arsenic adsorption onto the bulk shale and a value of approximately 3000 L/kg was calculated for arsenic adsorption onto the bulk shale/till mixture. These values are substantially higher than the value of 101.5 L/kg experimentally determined for arsenic adsorption onto the freshly formed iron oxides of the shale system. These numbers differ for a number of reasons. The Kd values calculated for the bulk shale and shale/till systems is really a desorption number. The amount of arsenic desorbing into the solution phase is what the Kd value represents when the total solid phase arsenic concentration is divided by the equilibrium solution arsenic concentration.

The Kd value determined from the spiking experiment represents adsorption and not desorption. In addition, using the total solid phase arsenic concentration to represent the adsorbed arsenic value or X over estimates the X value because not all of the solid phase arsenic is available for adsorption/desorption. Over estimating X will result in a higher Kd value. The method used to determine the Kd value would also make a large difference. In the spiking experiment the Kd was determined by taking the slope of the plot of adsorbed versus solution arsenic concentrations. The Kd for the bulk shale and shale/till systems was determined by simply dividing the total solid arsenic concentration by the solution concentration. Lastly, the Kd for the bulk shale and shale/till systems is larger because it represents all the phases that contribute to the adsorption/desorption of arsenic, and not just the adsorption onto the freshly precipitated iron oxide fraction of the shale represented by the Kd in the spiking experiment. In the literature, Kd values are closer to the experimentally determined value of 101.5 L/kg because the methods used to determine the Kd are similar to the method used in this study. All of the Kd values determined here are valid, as long as the limitations and differences in determining these numbers are known. The calculated bulk Kd values indicate that the higher pH shale/till system will have a lower Kd value. This means as pH is increased the amount of adsorbed arsenic will decrease and the amount of solution arsenic will increase. Partition coefficients are also useful in determining retardation coefficients (Rd) used in predicting the distance of contaminant (arsenic) movement in soil (shale). A higher retardation coefficient means less contaminant movement. The partition coefficient and the retardation coefficient are directly related. This means as the pH is increased the Kd will decrease as well as the Rd.

5.0 Conclusion

The concentration of aqueous arsenic released from the shale at the end of the 4-month equilibration under aerobic conditions as the system approached equilibrium is 1.2 μg/L. The predicted aqueous arsenic concentration under aerobic conditions at infinite time or when the system reaches equilibrium is between 1.2 and 0.6 μg/L. There was an overall drop in aqueous arsenic concentrations in the shale system under aerobic conditions over the 4-month equilibration. The concentration of aqueous arsenic released from the shale/till mixture under aerobic conditions at the end of the 4-month equilibration as the system approached equilibrium was 4.8 μg/L. The predicted aqueous equilibrium arsenic concentration in the shale/till mixture under aerobic conditions is between 4.8 and 9.4 μg/L. There was an increase in solution arsenic concentrations in the shale/till mixture under aerobic conditions over the 4-month equilibration. The concentration of solution arsenic in the shale/till system was 4X higher than the concentration in the shale system at the end of the 4-months. This study indicates the addition of lime to a Boundary soil raising pH to aid plant growth will increase the amount of aqueous phase arsenic.

The average concentration of aqueous arsenic in river water is 2 μg/L. Aqueous arsenic values above 2 μg/L are considered elevated. The current Canadian guideline value for arsenic in drinking water is 25 μg/L and in the United States the standard value is 10 μg/L. A solution arsenic concentration below 10 μg/L is not viewed as a public health threat in either country. These numbers indicate aqueous arsenic concentrations below 2 μg/L are extremely low and values between 2 μg/L and 10 μg/L are elevated but low and still pose no health risks. The concentration of aqueous arsenic in the shale system is extremely low (about 1 μg/L) and in the shale/till system is low (about 5 μg/L). This study indicates that the amount of arsenic released from the marine shale (surrogate for the Boundary soils) and from the shale/till mixture (surrogate for the Josephine soils) is low and should not

contribute to the build up of arsenic in the surrounding surface or groundwater provided the system remains oxidized.

Activity ratio diagrams theoretically predicted that the shale system was under-saturated with respect to solution arsenic over the 4-month equilibration under aerobic conditions and the precipitation of an arsenic solid phase was not controlling solution arsenic concentrations. The same prediction was made for the shale system at infinite time or equilibrium. An arsenic spiking experiment was conducted to test experimentally the previous theoretical prediction. The experiment determined and backed up the prediction that no arsenic solid phase was precipitating and controlling aqueous arsenic concentrations. Activity ratio diagrams constructed to represent the shale/till system over the 4-month equilibration and at equilibrium theoretically predicted that the precipitation of barium-arsenate was possible. However, an arsenic spiking experiment determined that the precipitation of an arsenic solid phase compound was not occurring in the shale/till mixture under aerobic conditions and did not control aqueous arsenic concentrations.

An arsenic super-saturation spike of 0.1 mole/L was added to the shale and shale/till systems to determine if the precipitation of an arsenic solid phase compound theoretically predicted from the activity ratio diagrams would occur. The precipitation of a white coprecipitated mixed solid did occur in the shale system after spiking. This compound contained arsenic, calcium, aluminum, and iron. This was not the compound/precipitate predicted from the activity ratio diagram, nor did the solution concentration of arsenic drop to the predicted concentration level. The precipitation of a solid phase compound was also predicted from the activity ratio diagram in the shale/till system at the arsenic solution concentration level achieved after spiking. The precipitation of an arsenic solid phase compound did not occur and the concentration of arsenic did not drop down to the predicted level.

A partition coefficient (Kd) of 101.5 L As/kg was calculated representing arsenic adsorption onto the freshly formed iron oxide fraction of the shale system. The predicted Kd for arsenic adsorption onto the bulk shale and bulk shale/till mixture was approximately 58,000 L As/kg shale and 3000 L As/kg shale/till mixture respectively. The addition of till to the shale and the subsequent increase in pH of the

new mixture decreases the amount of adsorbed arsenic and increases the amount of solution arsenic.

6.0 References

Alberta Environment 2000. Occurrence of arsenic in ground water near Cold Lake, Alberta.

Alberta Health and Wellness 2000: Characterization of arsenic in domestic wells in three areas of northern Alberta.

Backer, D. E., and Chesnin, L. 1975. Chemical monitoring of soils for environmental quality and animal and human health. Adv. Agron. 27:305-374.

Bates, M.N., A.H. Smith, and C. Hopenhayn-Rich. 1992. Arsenic ingestion and internal cancers: a review. Am. J. Epidemiol. **135(5)**:462-476.

Belzile, N., and Lebel, J. 1986. Capture of arsenic by pyrite in near-shore marine sediments. Chem. Geol. **54**:279-281.

Bohn, H. L. 1983. Ion activity products in soil solutions. Chapter 1, in Chemical mobility and reactivity in soil systems. Soil Sc. Soc. of America, Madison, WI.

Bohn, H. L., and Bohn, R. K. 1986. Solid activity coefficients of soil components. Geoderma **38**:3-18.

Bowell, R. J. 1994. Sorption of Arsenic by Iron Oxides and Oxyhydroxides in Soils. Appl. Geochem. **9**:279-286.

Bowen, H. J. M. 1979. Elemental Chemistry of the Elements. Academic Press, London and New York, pp. 60-61.

Bulmer, C. 1987. Nutrient imbalances of aspen poplar in acid sulfate soils in northwestern Alberta. M.Sc. University of Alberta, Edmonton, Alberta.

Bundy, L. G., and Bremner, J. M. 1972. A simple titrimtric method for determination of inorganic carbon in soils. Soil Sci. Soc. Amer. Proc. **36**:273-275.

Canada-Alberta Environmentally Sustainable Agriculture Agreement (CAESA) 1997: Alberta Farmstead Water Quality Survey. Prepared for CAESA Water Quality Monitoring Committee.

Canadian Council of Ministers of the Environment. 1999. Canadian Soil Quality Guidelines for the Protection of Environmental and Human Health: Arsenic (inorganic) (1997). In: Canadian Environmental Quality Guidelines. Manitoba Statutory Publications, Winnipeg, Manitoba. ISBN 1-896997-34-1.

Carapella, S. C. 1978. Arsenic and Arsenic Alloys. In M. Grayson and D. Eckroth (Eds.), Kirk-Othmer Encyclopedia of Chemical Technology, 3rd Edition. Wiley, New York, Vol. 3, pp. 243-250.

Carter, M.R., Ed. 1993. Soil Sampling and Methods of Analysis. Canadian Society of Soil Science. Lewis Publishers. CRC Press, Inc. Florida.

Coghlan, H. H. 1975. In T. K. Penniman and B. M. Blackwood (Eds.), Notes on the Prehistoric Metallurgy of Copper and Bronze in the Old World. Oxford University Press, Oxford.

Colbourn, P., Alloway, B. J., and Thorton, I. 1975. Arsenic and heavy metals in soils associated with regional geochemical anomalies in south-west England. Sci. Total Environ. **4**:359-363.

Davies, P. K., and Navrotsky, A. 1983. Quantitative correlations of deviations from ideality in binary and pseudobinary solid solutions. J. Sol. St. Ch. **46**:1-22.

Deer, W. A., Howie, R. A., and Zussman, J. 1978. An introduction to the rock forming minerals. Longman Group, London.

Derry, T. K., and Williams, T. I. 1961. A Short History of Technology. Oxford University Press, New York and Oxford.

Dove, P. M. and Rimstidt, J. D. 1985. The Solubility and Stability of Scorodite, $FeAsO_4$* $2H_2O$. Am. Mineral. **70**:276-278.

Dudas, M.J. and S. Pawluk. 1980. Natural abundances and mineralogical partitioning of trace elements in selected Alberta soils. Can. J. Soil Sci. **60**:763-771.

Dudas, M. J. 1987. Accumulation of native arsenic in acid sulphate soils in Alberta. Can. J. Soil Sci. **67**:317-331.

Dudas, M.J., Warren C. J., and Spiers, G. A. 1988. Chemistry of arsenic in acid sulphate soils of northern Alberta. Commun. Soil Sci. Plant Anal. **19**:887-895.

Emsley, J. 1985. Whatever Happened to Arsenic? New Sci. Dec., 1926 pp. 10-14.

Forbes, R. J. 1964. Studies in Ancient Technology. E. J. Brill, Leiden, The Netherlands.

Gimlette, J. D., and Desmond, J. 1981. Malay Poisons and Charm Cures. Oxford University Press, London.

Health Canada. 1996. Canadian Drinking Water Guidelines. Ottawa, ON

Hunter, D. 1978. The Diseases of Occupations. Hodder & Stoughton, London.

Iimura, K. 1981. Background contents of Heavy Metals in Japanese Soils. In K. Kitagishi and I. Yamane (Eds.), Heavy Metal Pollution in Soil of Japan. Jpn. Sci. Soc. Press, Tokyo, pp. 19-26.

Jones, D. 1982. The singular Case of Napoleons Wallpaper. New Sci. Oct., pp. 101-104.

Kittrick, J. A. 1966. Free energy of formation of kaolinite from solubility measurements. Am. Mineral. **51**:1457-1456.

Leonard, A. 1991. Arsenic. In E. Merian (Ed.), Metals and there Compounds in the Environment. VCH Verlagsgesellschaft, Weinheim, Germany.

Lindsay, W. L. 1979. Chemical Equilibria in Soils. John Wiley and Sons, New York.

Maeda, N., and Teshirogi, S. 1957. Studies on removing the bad effect of arsenic at paddy field. Nippon Dojo Hiryogaku Zasshi **28**:185-188.

Manning, B. A., and Goldberg, S. 1996. Modeling arsenic competitive adsorption on kaolinite, montmorillonite, and illite. Clays Clay Miner. **44**:609-623.

Manning, B. A., and Goldberg, S. 1997. Arsenic (3) and arsenic (5) adsorption on three California soils. Soil Sci. **162**:886-895.

McGeehan, S. L., and Naylor, D. V. 1994. Sorption and Redox Transformations of Arsenite and Arsenate in Two Flooded Soils. Soil Sci. Soc. Am. J. **58**:337-342.

McGeehan S. L. 1996. Arsenic sorption and Redox reactions relevance to transport and remediation. J. Environ. Sci. Health **A31**:2319-2336.

Mermut, A. R., Curtin, D. and Rostad, H. P. W. 1985. Micromorphological and submicroscopical features related to pyrite oxidation in an inland marine shale from east central Saskatchewan. Soil Sci. Soc. Am. J. **49**:256-261.

Meyer, E. V. 1975. A History of Chemistry- From Earliest Times to Present Day. Arno Press, New York.

Nriagu, J. O., and Azcue, J. M. 1990. Environmental sources of arsenic in food. Adv. Environ. Sci. Technol. **23**:103-127.

Pascal, P. 1958. Noveau Traite de Chemie Minerale, Vol. XI. Libraires de Academie de medecine, Paris.

Patrick, W. H., Gambrell, R. P., and Faulkner, S. P. 1996. Redox measurements of Soil. Methods of Soil Analysis. Part 3. Chemical Methods. Soil Science of America and American Society of Agronomy, Madison WI, USA.

Pawluk, S. and M. Dudas. 1978. Reorganization of soil materials in the genesis of an acid Luvisolic soil of the Peace River region, Alberta. Can. J. Soil Sci. **58**:209-220.

Pierce, M. L., and Moore, C. B. 1982. Adsorption of Arsenite and Arsenate on Amorphous Iron Hydroxide. Water Res. **16**:1247-1253.

Peterson, P. J., Benson, L. M., and Zieve, R. 1981. Metalloids, Sec. 3-Arsenic. In N.W. Lepp (Ed.), Effect of heavy metal Pollution on plants. Applied Science Publ., London, 1981, **Vol.1**, pp. 299-322.

Pugh, C. E., Hossner, L. R., and Dixon, J. B. 1981. Pyrite and marcasite surface area as influenced by morphology and particle diameter. Soil Sci. Am. J. **45**:979-982.

Pugh, C. E., Hossner, L. R., and Dixon, J. B. 1984. Oxidation rate of iron sulfides as affected by surface area, morphology, oxygen concentration, and autotrophic bacteria. Soil Sci. **137**:309-314.

Raade, G., Mladeck, M. H., Kristiansen, R., and Din, V. K. 1984. Kaatialaite, a New Ferric Arsenate Mineral from Finland. American Mineralogist **69**:383-387.

Raven, K. P., Jain, R. A., and Loeppert. 1998. Arsenite and Arsenate Adsorption on Ferrihydrite: Kinetics, Equilibrium, and Adsorption Envelopes. Environ. Sci. Technol. **32**:344-349.

Riewe, T. A., Weissbach, L., Heinen, and Stoll, R. 2000. Naturally-occurring arsenic in well water in Wisconsin. Water Well J. **54**:24-30.

Robins, R. G. 1981. The Solubility of Metal Arsenates. Metall. Trans. **12B**:101-109.

Ross, G. J., and Ivarson, K.C. 1981. The occurrence of basic ferric sulfates in some Canadian soils. Can. J. Soil Sci. **61**:99-107.

Ruhman, A. 1979. Mineralogical characteristics of soils from east central Alberta. M.Sc. Thesis, University of Alberta, Edmonton Alberta.

Sadiq, M., and Lindsay, W. L. 1981. Selection of standard Free Energies of Formation for use in Soil Chemistry, Arsenic. Supplement to Technical Bull. 134. Colorado State University Experiment Station. Fort Collins CO. pp. 21-372.

Sadiq, M., and Alam, I. 1996. Arsenic Chemistry in a Groundwater Aquifer from the Eastern Province of Saudi Arabia. Water Air Soil Pollut. **93**:117-136.

Sadiq, M. 1997. Arsenic Chemistry in Soils: An Overview of thermodynamic predictions and field observations. Water Air Soil Pollut. **93**:117-136.

Sandberg, G. R., and Allen, I. K. 1975. A proposed arsenic cycle in an agronomic ecosystem. ACS Symp. Ser. **7**:124-147.

Schwertmann, U. and Taylor, R. M. 1989. Iron oxides. *In* Minerals in soil environments. Eds. Dixon, J. B. and Weed, S. B. Soil Sci. Soc. Am. Madison, WI. 379-438.

Sheppard, M. I., and Thibault, D. H. 1990. Default soil solid/liquid partition coefficients, Kds, for four major soil types: A compendium. Health Phys. **59**:471-482.

Sheppard, S. C., Gaudet, C., Sheppard, P. M., Cureton, P. M. and Wong, M. P. 1992. The development of assessment and remediation guidelines for contaminated soils, a review of the science. Can. J. Soil Sci. **72**:359-394.

Sims, R. C. 1990. Soil remediation techniques at uncontrolled hazardous waste sites, a critical review. J. Air Waste Manage. Assoc. **40**:704-732.

Smith, E., Alam, I. 1999. Chemistry of arsenic in soils: 1. Sorption of arsenate and arsenite by four Australian Soils. J. Environ. Qual. **28**:1719-1726.

Sposito, G. 1981. The thermodynamics of soil solutions. Oxford University Press, New York.

Stahl, R. S., Fanning, D. S., and James, B. R. 1993. Geothite and jarosite precipitation from ferrous sulfate solutions. Soil Sci. Soc. Am. J. **57**:280-282.

Takahashi, W., Pfenninger, K., and Wong, l. 1983. Urinary arsenic, chromium, and copper levels in workers exposed to arsenic-based wood preservatives. Arch. Environ. Health **38:**209-214.

Thompson, D. V. 1956. The materials and techniques of medieval painting. Dover, New York.

USEPA. 1990. Statistics of aquifer material properties and empirical pH-dependent partitioning relationships for As(3), As (5), Ba(2), Be(2), Cd(2), Cr(6), Cu(2), Hg(2), Ni(2), Pb(2), Sb(5), Ti(1), and Zn(2). Athens, GA.

Van Breemen, N. 1982. Genesis, morphology and classification of acid sulfate soils in coastal plains. In: Acid sulfate weathering. SSSA special publication no. 10. Eds. J. A. Kittrick, D. S. Fanning, L. R. Hossner. Madison, Wis. pp.95-108.

Vaslow, F., and Boyd, G. E. 1952. Thermodynamic of coprecipitation: Dilute solid solutions of AgBr in AgCL. J. Amer. Chem. Soc. **74**:4691-4695.

Vink, B. W. 1996. Stability Relations of Antimony and Arsenic Compounds in the Light of Revised and Extended Eh-pH Diagrams. Chem. Geol. **130**:21-30.

Warner, J. E., and Solomon, K. R. 1990. Acidity as a factor in the leaching of copper, chromuim and arsenic from CCA-treated dimension lumber. Environ. Toxicol. Chem. **9**:1331-1337.

Warren, C. J. 1991. Weathering, trace elements, and smectite stability in extremely acid soil environments. Doctor of Philosophy Thesis, University of Alberta, Edmonton, Alberta.

Waychunas, G. A., and Moore, B. 1993. Surface chemistry of ferrihydrite: Part 1: EXAFS studies of the geometry of coprecipitated and adsorbed arsenate. Geochim, Cosmochim. Acta **57**:2251-2269.

Webb, J. L. (1966). Arsenicals. Enzyme and Metabolic Inhibitors. Academic Press, New York, **Vol. 3**,pp. 595-790.

Wilkie, J. A., and Hering, J. G. 1996. Adsorption of arsenic onto hydrous ferric oxides: effects of adsorbate/adsorbent ratios and co-occurring solutes. Coll. Surf. **107**:97-110.

Woolson, E. A., Axley, J. H., and Kearney, P. C. (1971). Correlation between available soil arsenic, estimated by six methods, and response of corn. Soil. Sci. Soc. Am. Proc. **35**:101-105.

Woolson, E. A., Axley, J. H., and Kearney, P. C. (1973). The chemistry and phytotoxicity of arsenic in soil: 2. Effects of time and phosphorus. Soil Sci. Soc. Am. Proc. **37**:254-259.

Wu, S., Zhao, W. Y., Feng, X., and Wittmeier, A. 1996. Application of Induced Coupled Plasma Mass Spectrometry for Total Metal Determination in Silicon-containing Solid Samples Using the Microwave-assisted Nitric Acid-Hydrofluoric Acid-Hydrogen Peroxide-Boric Acid Digestion System. J. Anal. Atomic Spec. **11**:287-296.

Xu, H., Allard, B., and Grimvall, A. 1991. Effects of acidification and natural organic materials in the mobility of arsenic in the environment. Water, Air, Soil pollution. **58**:269-278.

Zou, B. J. 1986. Arsenic in Soil. Turangxue Jinzhan **14**:8-13.

Appendix 1. Change in chemical parameters over time for experiment 1(marine shale) and experiment 2 (marine shale and till).

Mean Data Equilibration Experiment
1- Marine Shale

time (days)	sample (TM)	Na mg/L	Mg mg/L	Al ug/L	K mg/L	Ca mg/L	Mn ug/L	Fe ug/L	As ug/L	Mo ug/L	Ba ug/L	SO4 mg/L	pH	redox (mV)	E.C (dS/m)
1	1	1.1	3.1	59553.0	18.5	594.0	338.0	6323.0	2.3	0.4	12.8	11557.0	3.0	686.7	2.4
2	2	1.0	2.9	55209.0	14.7	584.0	319.0	5359.0	2.8	0.4	14.2	11089.9	3.1	669.7	2.4
4	3	4.2	6.2	52491.0	12.3	577.0	320.0	6729.0	6.8	0.3	9.4	2368.6	3.1	645.7	2.0
8	4	3.9	8.9	56133.0	7.5	553.0	389.0	113056.0	3.3	0.1	7.9	2529.7	3.0	521.0	2.8
16	5	2.9	5.3	45026.0	4.0	543.0	446.0	426890.0	3.7	0.2	6.2	3020.9	3.1	480.3	2.2
32	6	2.7	8.6	86659.0	1.1	500.0	462.0	111720.0	4.0	0.5	4.7	1930.6	2.7	614.3	2.8
48	7	1.9	6.8	86920.0	0.4	485.0	443.0	30257.0	3.3	0.5	6.8	1842.1	2.6	691.0	2.5
64	8	1.9	7.5	87983.3	0.2	553.5	575.8	21891.1	3.3	0.5	6.3	1826.9	2.7	790.0	2.7
128	9	1.8	7.5	88384.0	0.4	529.0	403.0	13823.0	1.2	0.2	6.8	1951.0	2.8	789.7	2.5

Mean Data Equilibration Experiment
2- Marine Shale and Till

time (days)	Sample (TP)	Na ug/L	Mg mg/L	Al ug/L	K ug/L	Ca mg/L	Mn ug/L	Fe ug/L	As ug/L	Mo ug/L	Ba ug/L	SO4 mg/L	HCO3- mg/L	pH	redox (mV)	E.C (dS/m)
1	1	3273.9	29.8	5.6	5076.1	702.4	98.6	<50	1.8	3.8	9.5	1494.1	486.0	6.1	266.0	1.2
2	2	3296.0	31.0	5.8	4862.7	702.7	94.1	<50	2.3	4.2	10.0	1466.9	526.5	6.2	382.3	1.4
4	3	3465.1	33.1	4.6	5018.4	700.6	90.1	<50	2.9	4.7	9.3	1476.0	496.1	6.2	343.0	1.4
8	4	3064.4	33.6	2.8	3985.0	592.6	92.8	49.8	1.8	5.7	7.8	1455.2	394.8	6.5	334.3	1.0
16	5	4198.9	43.0	30.8	4648.4	560.7	85.1	112.4	2.3	7.5	7.5	1495.4	222.7	6.8	304.7	1.3
32	6	3917.7	37.8	3.0	2225.7	658.8	128.6	<25	2.6	9.9	6.8	1602.0	141.7	6.9	268.3	1.2
48	7	2811.9	31.6	4.6	2456.0	599.0	284.0	<15	2.5	8.2	7.0	1654.6	86.1	6.7	252.7	1.2
64	8	2901.1	38.0	314.0	2517.0	608.0	498.0	<15	2.9	8.2	14.0	1658.3	77.2	6.7	232.3	1.3
128	9	1962.0	35.7	225.5	1458.0	599.5	476.5	<25	4.8	17.1	13.7	1548.7	92.6	6.9	373.0	1.1

Appendix 2. Change in major ion concentrations in spiking experiment 2,before and after the arsenic spike (0.1mol/L) in the shale and shale/till systems.

Mean data-spiking experiment 2-
marine shale

	Na ug/L	Mg ug/L	Al ug/L	K ug/L	Ca ug/L	Mn ug/L	Fe ug/L	As ug/L	Mo ug/L	Ba ug/L
before spike	4867	10744	43722	21756	583647	260	2994	3.31	B.D	4.29
after spike	3766173	9577	484	25160	514336	33	53	6783047	B.D	B.D

Mean data-spiking experiment 2-
marine shale and till

	Na ug/L	Mg ug/L	Al ug/L	K ug/L	Ca ug/L	Mn ug/L	Fe ug/L	As ug/L	Mo ug/L	Ba ug/L
before spike	25143	44200	7.23	7328	651372	232	99.7	B.D	6.89	8.77
after spike	3554550	40580	3.43	10759	631424	47.2	50.8	6870940	7.36	7.16

Note- B.D indicates concentrations were below detection limits